

# A Review of Aeronautical Fatigue Investigations in Brazil

International Committee on Aeronautical Fatigue (ICAF)  
Helsinki – Finland – June, 2015

Prepared by:

**Carlos E. Chaves**

On behalf of:

**Fatigue, Fracture and Structural Integrity Committee**

**Brazilian Society of Engineering and Mechanical Sciences - ABCM**



# A Review of Aeronautical Fatigue Investigations in Brazil ICAF 2015 – Helsinki - Finland



## SUMMARY

This report presents the review of fatigue investigations related to aeronautics performed in Brazil during the years 2013 to 2015. Its contents will be presented during the 34<sup>th</sup> ICAF (International Committee of Aeronautical Fatigue) Conference to be held in Helsinki, Finland, in June 01 to 02, 2015.

## CONTENTS

1. INTRODUCTION .....	7
2. ANALYSIS AND SIMULATION .....	9
3. METALLIC MATERIALS – FATIGUE AND FRACTURE PROPERTIES .....	13
4. METALLIC MATERIALS – STRUCTURES.....	19
5. COMPOSITE MATERIALS.....	25
6. BONDING.....	32
7. STRUCTURAL HEALTH MONITORING.....	40
8. REPAIRS.....	49
9. MISCELLANEOUS.....	49
10. REFERENCES.....	51

## ABBREVIATIONS

ABCM	Associação Brasileira de Engenharia e Ciências Mecânicas (Brazilian Society of Engineering and Mechanical Sciences)
AE	Acoustic Emission
AMM	Airplane Maintenance Manual
ANAC	Agência Nacional de Aviação Civil (Brazilian Aviation Agency)
ASTM	American Society for Testing and Materials
COBEM	Congresso Internacional de Engenharia Mecânica (International Congress of Mechanical Engineering)
CTA	Centro Tecnológico Aeroespacial (Aerospace Technological Center)
CVM	Comparative Vacuum Monitoring
DCB	Double Cantilever Beam
DET	Detailed Visual Inspection
DIC	Digital Image Correlation
EMB	Embraer
EMI	Electro-Mechanical Impedance
ERJ	Embraer Regional Jet
FAB	Força Aérea Brasileira (Brazilian Air Force)
FCG	Fatigue Crack Growth
FDG	Fatigue Disbond Growth
FE	Finite Element
FML	Fiber Metal Laminate
FSFT	Full-Scale Fatigue Test
FSW	Friction Stir Welding
GFEM	Global Finite Element Method
GVI	General Visual Inspection
HLUP	Hand Lay-Up
IPT	Instituto de Pesquisas Tecnológicas (Technology Research Institute)
ITA	Instituto Tecnológico de Aeronáutica (Aeronautical Institute of Technology)

LW	Lamb Waves
MMB	Mixed-Mode Bending
MSD	Multi-Site Damage
OEM	Original Equipment Manufacturer
S/A	Sociedade Anônima (Corporation)
SG	Strain Gage
SHM	Structural Health Monitoring
SLJ	Single Lap Joint
SP	São Paulo State
S-SHM	Scheduled Structural Health Monitoring
UNICAMP	Universidade de Campinas (University of Campinas)
UNIFEI	Universidade Federal de Itajubá (Federal University of Itajubá)
USP	Universidade de São Paulo (University of São Paulo)
VaRTM	Vacuum Assisted Resin Transfer Molding

## INDEX OF FIGURES

Figure 1 - Splitting Method – Overview. ....	10
Figure 2 – Outline of the GFEM. ....	10
Figure 3 – Butt Joint Configurations Analyzed.....	11
Figure 4 – Example of Fastener 3D Modelling. (a) 3D view; (b) Cross Section Showing Deformation and Contact (Rivet to Skin) Surfaces. ....	11
Figure 5 – Butt Joint Analysis - Experimental Correlation.....	12
Figure 6 – Example of Comparison of Strain Values (Numerical vs. Experimental) for Various SG Locations. ....	12
Figure 7 – Effect of Salt-water Fog on Fatigue Crack Nucleation of Al and Al-Li Alloys....	14
Figure 8 – Comparison of Crack Propagation Behavior for AA2198-T851 (results from Ref. [5]), AA7050-T7451, AA2524-T3 and AA2050-T84 (results from Ref. [6])......	15
Figure 9 – Comparison of Crack Propagation Behavior for AA7050-T7451 (results from Ref. [6]) and AA2050-T84 (results from Ref. [8]). ....	16
Figure 10 – Comparison of Fracture Toughness for AA7050-T7451 (results from Ref. [6]) and AA2050-T84 (results from Ref. [8])......	16
Figure 11 - Corrosion Fatigue Test (a) MTS Machine and (b) the Scheme of Crack Encapsulation System. ....	17
Figure 12 - Fatigue Fracture under TWIST Flight Sequence at (a) Air Environment, (b) 3.5% NaCl, (c) 5.0% NaCl.....	18
Figure 13 - Fatigue Fracture under FALSTAFF Flight Sequence at (a) Air Environment, (b) 3.5% NaCl, (c) 5.0% NaCl.....	18
Figure 14 – Legacy 500 (EMB-550) Executive Jet. ....	21
Figure 15 – Legacy 500 (EMB-550) Full-Scale Fatigue Test Overview. ....	21
Figure 16 – Lower Skin Panel Crack Growth Test Device – General View.....	22
Figure 17 – Crack Growth Results for Skin Panel Specimens.....	22
Figure 18 – ERJ-190 Full-Scale Fatigue Test Specimen.....	23
Figure 19 – Fuselage Barrel Fatigue Test Specimen and Rig. ....	24
Figure 20 - Advanced Wing Spar Concept. ....	25
Figure 21 – Outline of Durability Test Setup.....	26
Figure 22 – Predicted Buckling Loads/Mode Shapes. ....	26
Figure 23 - Load .vs. Displacement Curves Obtained from the Durability Tests. ....	27

Figure 24 - Dimensions of DCB Specimens used for Interlaminar Fracture in Mode I Characterization (h = 3.04 mm).....	28
Figure 25 - Curve $G_I$ Versus Delamination Extension for Specimens Tested at 25°C. ....	29
Figure 26 - Loading Configuration for DCB Testing under Mixed Mode I/II.....	30
Figure 27 - Flowchart for Fatigue Limit Strain Determination.....	32
Figure 28 – Arcan Tests and Simulation. ....	34
Figure 29 – Comparison Between Tests and Numerical Simulation – Mixed Mode.....	34
Figure 30 – Bonded Repair - Test.....	35
Figure 31 – Bonded Repair - Numerical Analysis.....	35
Figure 32 – Bonded Repair Crack Growth – Experimental vs. Numerical Results.....	36
Figure 33 – Fatigue Disbond Growth Behavior. Pure Mode I and II.....	38
Figure 34 – Fatigue Disbond Growth Behavior. Mixed-Mode - FCG.....	38
Figure 35 – Model predictions for the MM - FCG set of data. ....	39
Figure 36 – Single Lap Joints - Specimen Details. ....	39
Figure 37 – Fatigue Disbond Growth Rate Results. ....	39
Figure 38 – FDG Prediction for Both Disbond Tips of a SLJ.....	40
Figure 39 – Specimens 01 and 02 with PZTs Bonded.....	41
Figure 40 – Damage Identification Spectrogram at 200kHz Using Direct Image Path with Damage Simulator Positioned on the Plate and Sensor Positioned on the Stringer. ....	42
Figure 41 – Example of Signal Response of the Sensor Network with 3 PZT Positioned on the Stringer with Higher Scatter at 200kHz. ....	43
Figure 42 – Example of a Crack Detected by a CVM Sensor in the Metallic Barrel Test. (a) CVM Sensors Installed Around Rivets; (b) Sensors Removed and Dye Penetrant Testing Confirmed Presence of a 2mm Crack. ....	44
Figure 43 – CVM Sensors Installed in Various Regions of the E-Jets Full-Scale Fatigue Tests.....	45
Figure 44 – LW Sensors Applied to the E-Jets Full-Scale Fatigue Test.....	45
Figure 45 – Flight Test Aircraft Where CVM and LW Sensors Were Installed. ....	46
Figure 46 – Examples of CVM Sensors Installed in the Flight Test Aircraft. ....	46
Figure 47 – LW Sensors Applied to Flight Tests, Embraer-190 Aircraft. (a) Trailing Wing Box; (b) Passenger Door. ....	47
Figure 48 – Fuselage Panel in the E-Jets FSFT Monitored by Acoustic Emission.....	47
Figure 49 – Examples of Acoustic Emission: (a) Barrel Test; (b) Coupon Test.....	48

## 1. INTRODUCTION

This document was prepared in order to summarize fatigue and fracture investigations related to aeronautics performed in Brazil during the past two years. Its contents will be presented in the 34<sup>th</sup> ICAF (International Committee of Aeronautical Fatigue) Conference to be held in Helsinki, Finland, in June 01 to 02, 2015.

Although all research work that is presented in the sections that follow refers to the past two years, due to the fact that this is the first Brazilian report submitted to the ICAF, it seems appropriate to include a short discussion about the origins of the aeronautic industry in Brazil in the introductory section.

Brazil has a long tradition in aeronautics since Alberto Santos Dumont performed his first flight with a fixed wing aircraft, called 14-Bis, in Paris in 1906. After Santos Dumont, many Brazilians engaged in a series of efforts to license products and to create joint ventures with foreign manufactures.

Later, in 1946 the Brazilian Air Force planned and established the Aerospace Technological Center (CTA) in São José dos Campos, a city located about one hundred kilometers from São Paulo. This technical center, when conceived, included a superior education center, called Aeronautical Institute of Technology (ITA), inaugurated in 1950, that was created in partnership with the Massachusetts Institute of Technology (MIT). More details about the foundation of CTA and ITA are available in References [1] and [2]. Today ITA is one of the most important engineering schools in Brazil, and some of the works presented along this report were developed by fellows from that institution.

From the CTA, Embraer Aircraft Manufacturer was created in 1969. The first aircraft produced by Embraer were turboprops ordered by the Brazilian Air Force (FAB). Training jets were built in partnership with the Italian manufacturer Aermacchi during the seventies. Later many products were developed and manufactured by Embraer while it belonged to the Brazilian Government. After being privatized in 1994, Embraer started a growth process made possible by successful combination of its solid technological and industrial culture developed throughout the years with the strong business culture brought by its stakeholders, and driven by the ERJ 145 family project. In the following years, with the launch of the EMB 170/190 family, the Legacy Executive aircraft, the Intelligence, Surveillance and Reconnaissance family of defense products, and the ALX/Super Tucano, Embraer has significantly expanded its presence, reaching a top position in the world's aviation market. Nowadays it is the third manufacturer of commercial aircraft of the world (Refs. [1] and [2]).

Although Embraer aircraft relies on a large amount of systems developed by a range of different suppliers from around the world, their airframe have been always designed, developed, tested and certified in Brazil.

Further, during the last decades Brazil has developed and manufactured other aeronautical products, such as helicopters, landing gears, and others. Helibras is an Airbus Helicopter facility located in the city of Itajubá, originally founded from CTA in 1978. Other foreign companies, such as Boeing and Airbus, have established research centers in São José dos Campos during the last decade.

To remain competitive, Brazilian aeronautic industry counts with the cooperation of a range of universities and research institutes. During the last decade, this cooperation has increased together with the growth of industry.

The following institutions have cooperated during the past years with research works on fatigue and fracture mechanics related to aeronautical products, and many of them have works added to this review:

- Brazilian Society of Engineering and Mechanical Sciences – ABCM – São Paulo - SP
- Brazilian Air Force Aeronautical Technical Center (CTA) – São José dos Campos - SP
- Technology Research Institute (IPT) – São Paulo – SP
- University of São Paulo (USP) – Campus of São Carlos – São Carlos – SP
- University of São Paulo (USP) – Campus of Lorena – Lorena - SP
- University of Campinas (UNICAMP) – Campinas - SP
- Aeronautical Institute of Technology (ITA) – São José dos Campos – SP
- Federal University of Itajubá (UNIFEI) – Itajubá – MG
- Embraer S/A – São José dos Campos – SP

Further, some works to be presented were developed in cooperation with foreign institutions, from which the following are mentioned here:

- Delft University – Delft – The Netherlands
- Aleris Rolled Products – Koblenz – Germany
- Helmholtz-Zentrum Geesthacht (HZG) – Germany

The author would like to thank to all partners from the Academy who collaborated with this compilation, some of which will be cited during the report. The author is also grateful to Mr. Fernando F. Fernandez and to Dr. Giorgia T. Aleixo, from the Technological Development Department of Embraer, for their help and continuous support during the organization of this work.

## 2. ANALYSIS AND SIMULATION

The main collaboration regarding simulation refers to the GFEM method development and its potential application to analytical evaluation of multiple site damage problems. This work has been carried out by Professor Sergio Proença and co-workers (Ref. [3]), from the University of São Paulo.

The Generalized Finite Element Method (GFEM) and a Decomposition Method for fracture mechanics problems (“Splitting Method”) are combined aiming the development of an accurate and robust numerical tool for structural analysis accounting for multi-site damage (MSD) evolution in different scales.

The methodology for modeling multi-site damage is based on the Splitting Method, which differs from similar decomposition methods not only by its ability to capture interactions among cracks and mathematical supported accuracy but also because it consists of a non iterative procedure.

In short, the splitting scheme decomposes the original problem in a set of global crack free problems conceived to account for the boundary conditions and crack interactions and a set of isolated crack problems aiming to capture local effects, as shown in Figure 1. The stress free condition on the crack surfaces is imposed when superposing the sub-problems.

The ability of the Generalized Finite Element Method to lead with fracture mechanics problems is well known and this feature can be efficiently explored on multi-site damage problems. In particular, GFEM can be applied to solve the local problems of the splitting method. This is a first aspect to be addressed in the works being developed. In spite that the formulation is designed to a three-dimensional approach the initial numerical implementations are devoted to two-dimensional problems.

The global-local version of the GFEM, referenced here as GFEM-GL and outlined in Figure 2, is extended to multi-site damage analysis. The basic objective is to affront problems where damage of different sizes and locations must be considered. Thus, multi-scale analysis is the second aspect addressed. Accordingly, the numerical solutions of small scale multi-site damage problems are used to provide enrichment functions for the large scale analysis.

SPLITTING METHOD

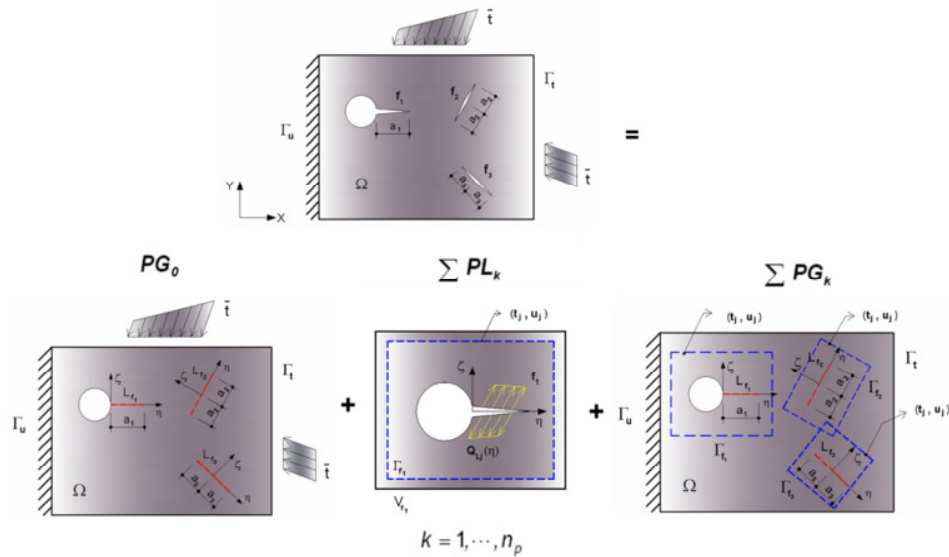


Figure 1 - Splitting Method – Overview.

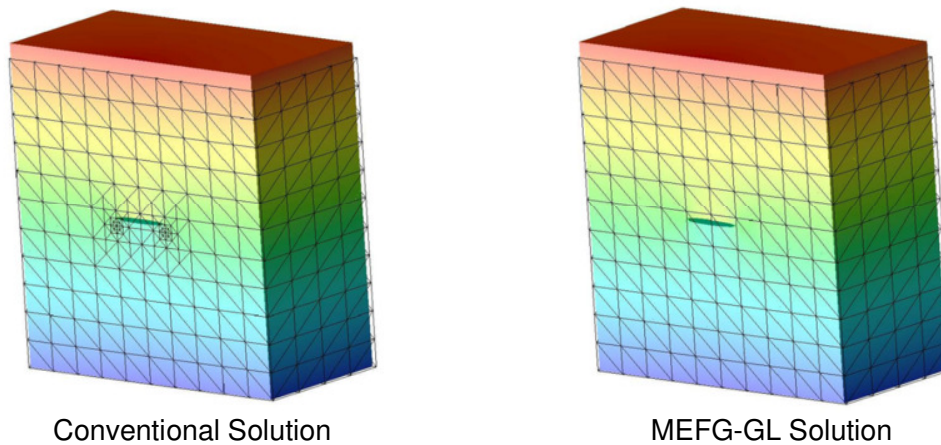


Figure 2 – Outline of the GFEM.

Regarding simulation of structural components, a comprehensive work on simulation of fuselage joints was developed by André Carunchio and co-workers (Ref. [4]), from the Technology Research Institute (IPT). Their work presented an investigation on the modeling of riveted joints using 3D finite elements and contact tools, as analytic contact, to improve the results accuracy. The main objective of this work was to recommend best practices to conduct a 3D FE analysis of a riveted butt joint configuration, and to identify

which parameters and effects must be mainly considered to reach accurate and reliable results.

Two types of configuration were analyzed, one corresponding to a strip with six solid countersunk rivets and one corresponding to a panel with six rows of five solid countersunk rivets, as shown in Figure 3. For each of these configurations, different cross sections and manufacturing characteristics were evaluated.

Figure 4 shows some examples of meshes developed for modeling the fastened joints in this work.

The accuracy of the FEM models developed was verified by strain gages, photoelasticity and digital image correlation, as outlined in Figure 5. Figure 6 shows the strain gage correlation for various locations under a specific loading condition.

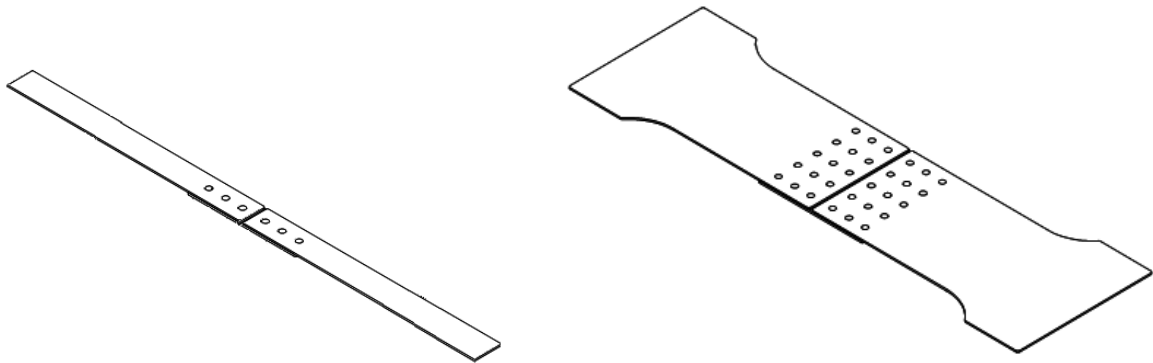


Figure 3 – Butt Joint Configurations Analyzed.

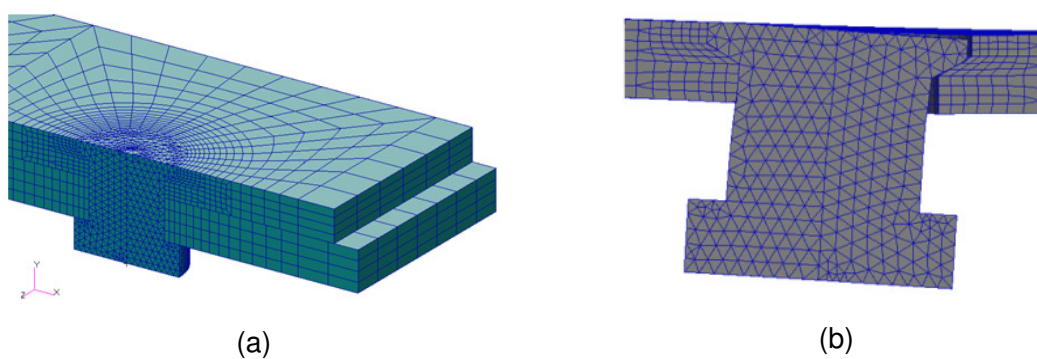
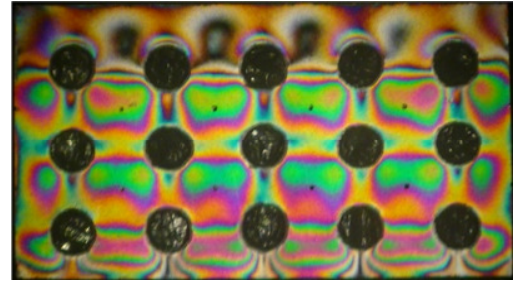
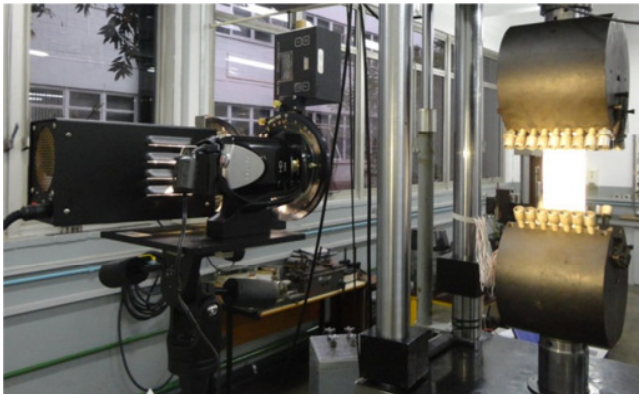
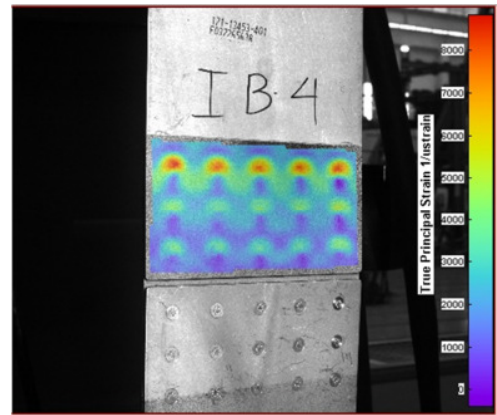


Figure 4 – Example of Fastener 3D Modelling. (a) 3D view; (b) Cross Section Showing Deformation and Contact (Rivet to Skin) Surfaces.



(a) Photoelasticity



(b) Digital Image Correlation (DIC)

Figure 5 – Butt Joint Analysis - Experimental Correlation.

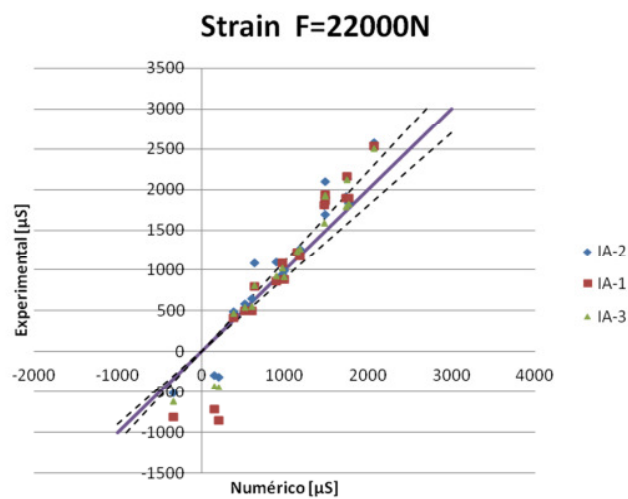


Figure 6 – Example of Comparison of Strain Values (Numerical vs. Experimental) for Various SG Locations.

Recommendations on the model hierarchical level, verification of the fastener material properties (in order to correct for the fastener flexibility after hardening) fastener modeling, and contact (discrete or analytic) resulted from this work. The authors also emphasized the importance of modeling friction and squeezing force for situations where the applied load increases.

The second part of this work, including fatigue test results for the same joint configurations being analyzed, will be presented during the 23<sup>rd</sup> International Congress of Mechanical Engineering (COBEM 2015 - Rio de Janeiro - RJ), supported by the Brazilian Society of Engineering and Mechanical Sciences (ABCM), in to be held in December of 2015.

Other works including numerical analysis will be presented in Sections 5 (Composite Materials), 6 (Bonding) and 8 (Repairs) of this report.

### 3. METALLIC MATERIALS – FATIGUE AND FRACTURE PROPERTIES

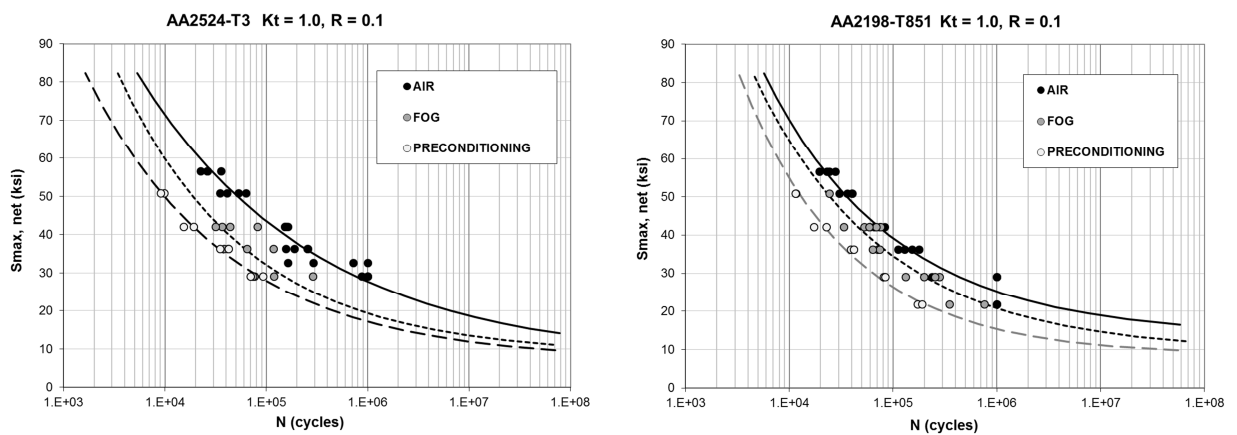
Many investigations have been done by Dr. Waldek Bose Filho and his team, from the Department of Materials Engineering, University of São Paulo (USP), during the past years regarding fatigue properties of recently developed aluminium alloys, from which the following will be cited:

*Effect of Salt-water Fog on Fatigue Crack Nucleation of Al and Al-Li Alloys (Ref. [5]):* Fatigue and corrosion-fatigue tests were performed to quantify the fatigue properties of AA2524-T3 and AA2198-T851 Al alloys. High cycle axial fatigue tests were carried out under air and salt-water fog conditions. Figure 7(a) schematically shows the test setup. In air, the specimens were fatigue tested at a frequency of 50 Hz, using specimens with and without preconditioning in a salt spray chamber (5.0 wt% NaCl) at 35°C, and for the corrosion fatigue condition, the tests took place at a frequency of 30 Hz in a salt-water fog condition (3.5 wt% NaCl). In all cases a sinusoidal waveform was used and a stress ratio  $R=0.1$  was applied.

Figure 7(b) shows the *S-N* curves obtained for all conditions evaluated. The results indicated that the saline environment had a deleterious effect on the fatigue life of the two aluminium alloys. AA2524-T3 exhibited a better fatigue strength than AA2198-T851 when fatigue tested in air. However, considering the corrosion fatigue test in a saline fog environment an inverse behavior was observed with the AA2198-T851 exhibiting higher fatigue strength.

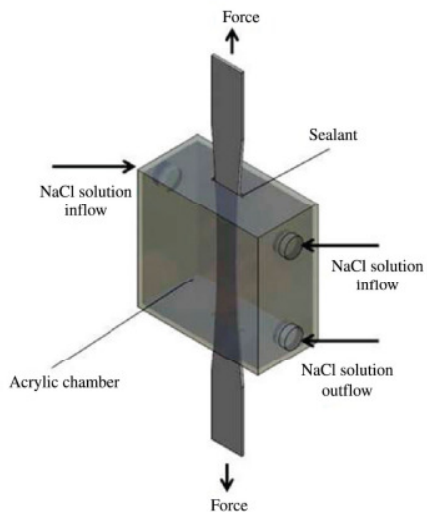
*Fatigue Behavior of Al-Li AA2050-T84 Alloys (Ref. [6]):* Many novel Al-Li alloys are becoming more attractive for aeronautic structures due to their low density, high elastic modulus, increased mechanical strength and good corrosion resistance. The aim of this work was to study the fatigue strength of the new Al-Li alloy AA2050-T84, considering both the nucleation and propagation fatigue lives. In the first case the effect of the stress

concentrator factor ( $k_t$ ) and the stress ratio ( $R$ ) were evaluated, while in the propagation life the effect of rolling direction and stress ratio  $R$  were considered. The results from the propagation life showed that in both L-T and T-L directions and for a constant  $K$ , higher  $R$  induced larger fatigue crack propagation rate. Considering a constant  $R$ , the T-L direction presented a larger Paris exponent ( $m$ ), which is an indicative of higher crack propagation rate. Also, larger  $R$  resulted in larger  $m$ , independently of the rolling direction. The Forman equation was able to take into account the  $R$  effect on the crack propagation rate for this Al-Li alloy. Considering the more traditional Al alloys from the 2XXX and 7XXX families, and the new Al-Li alloys AA2198, the AA2050 presented a quite similar fatigue behavior.

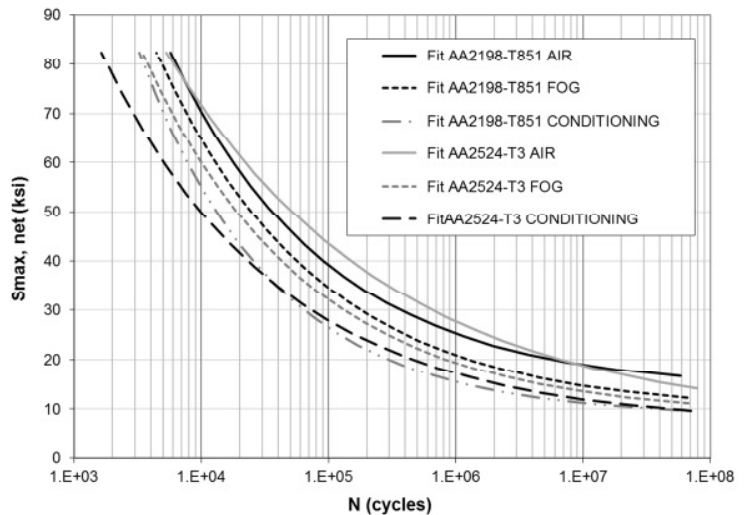


(a) S-N Curve – AA2524-T3

(b) S-N Curve – AA2198-T851



(c) Schematic view of the experimental setup for corrosion fatigue tests.



(d) Comparison of S-N curves of AA2524-T3 and AA2198-T851 aluminium alloys in tested under different environments and specimens conditions.

Figure 7 – Effect of Salt-water Fog on Fatigue Crack Nucleation of Al and Al-Li Alloys.

Figure 8 shows the comparison of crack growth behavior in Region II for the Al-Cu alloy AA2524-T3, for the Al-Zn alloy AA7050-T7451, and for the Al-Li alloys AA2198-T851 and AA2050-T84.

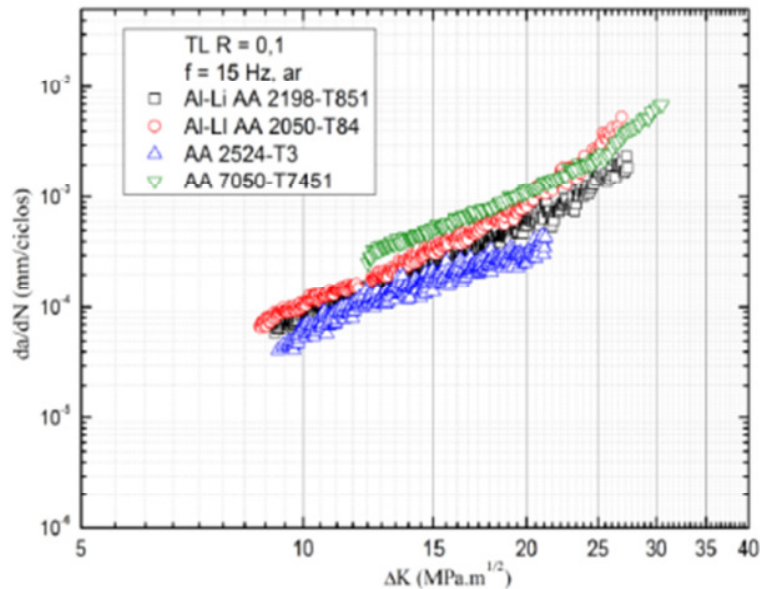


Figure 8 – Comparison of Crack Propagation Behavior for AA2198-T851 (results from Ref. [5]), AA7050-T7451, AA2524-T3 and AA2050-T84 (results from Ref. [6]).

*Microstructural Analysis, Fracture Toughness and Fatigue Life in AA7050-T7451 and AA2050-T84 (Refs. [6] and [8]):* In these studies, the influence of temperature in fracture toughness  $K_{Ic}$ , and in the crack propagation rate,  $da/dN$ , were evaluated by comparing AA7050-T7451 and AA2050-T84 alloys, Figure 9. The microstructures of these alloys were analyzed with optical, electron scanning and electron transmission microscopies. Tensile tests were performed at room temperature and  $-54^{\circ}\text{C}$ . The results of  $K_{Ic}$  tests, Figure 10, conducted according to ASTM E399, showed that at room temperature the AA2050-T84 has higher fracture toughness, but that for low-temperature AA7050-T7451 presents higher fracture toughness. For the R curve, it was found that in L-T direction the alloy AA2050-T84 has higher crack propagation resistance when compared to AA7050-T7451, while in T-L direction, the opposite behavior was observed. Regarding the FCG tests, the AA2050-T84 had a lower crack propagation rate than the AA7050-T7451 at  $-54^{\circ}\text{C}$ . In room temperature, the rate of propagation of the AA7050-T7451 was lower with respect to the AA2050-T84.

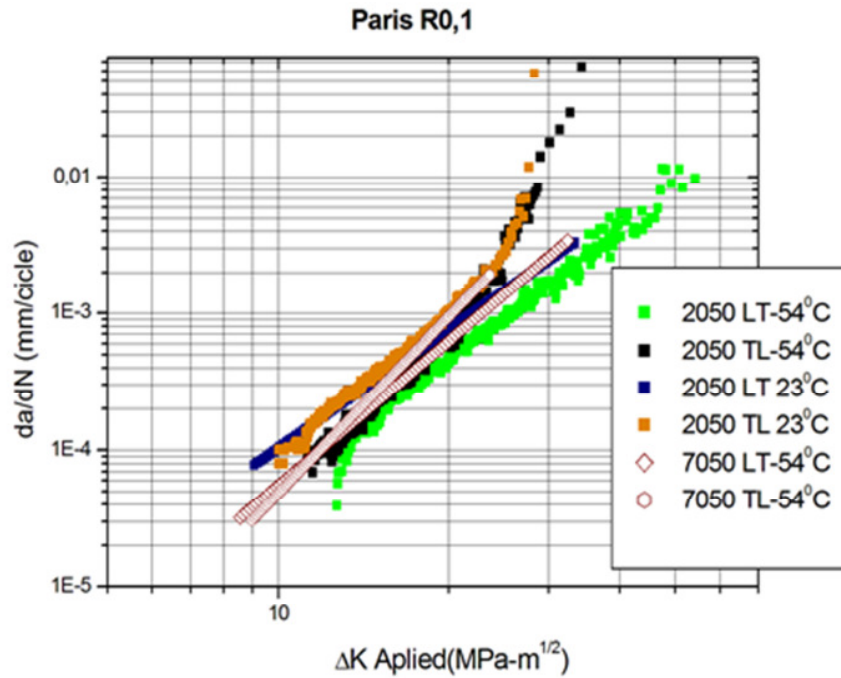


Figure 9 – Comparison of Crack Propagation Behavior for AA7050-T7451 (results from Ref. [6]) and AA2050-T84 (results from Ref. [8]).

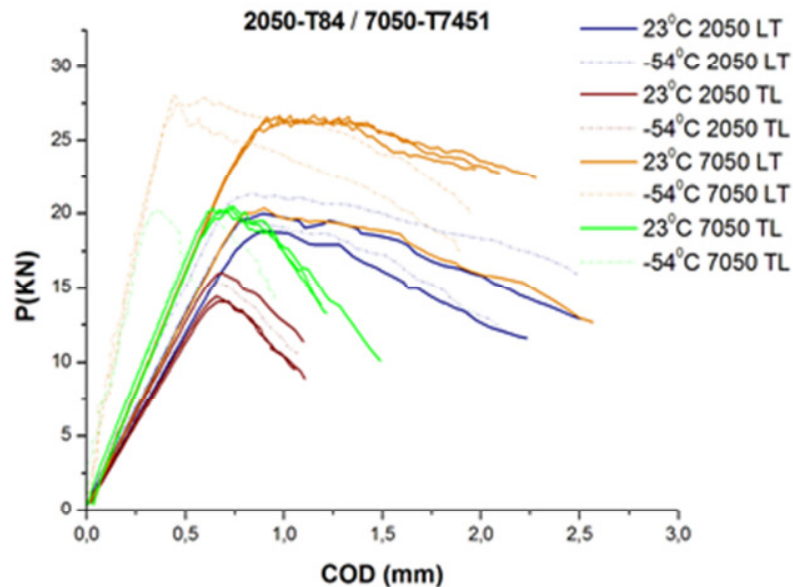


Figure 10 – Comparison of Fracture Toughness for AA7050-T7451 (results from Ref. [6]) and AA2050-T84 (results from Ref. [8]).

*Corrosion Fatigue Crack Growth of AA7475-T7351 Aluminium Alloy under Flight Simulation Loading (Ref. [9]):* Corrosion crack propagation experiments were carried out on specimens of AA7475-T7351. Variable amplitude tests were performed with flight-simulated spectrum TWIST and FALSTAFF exposed to air and saline environment.

Fatigue crack growth tests used M(T) specimens in T-L direction, dimensions (244x100x3mm), center notch 10mm and pre crack 1mm ( $2a=2\text{mm}$ ). The tests were performed at room and saline environment of 3.5% and 5.0% NaCl on MTS dynamic test machine, Figure 11. The 3.5% NaCl was chosen as one of the environments because of the composition of seawater and 5.0%NaCl was chosen because this composition is recommended for corrosion acceleration tests. The crack size was determined by the electrical-potential method.

The results showed that fatigue crack propagation life of specimens tested on saline environment were longer than specimens tested on air environment. The fatigue surfaces of specimens tested on saline environment examined in the SEM showed oxide and Na crystals in the wake of crack, which can promote retardation of crack propagation.

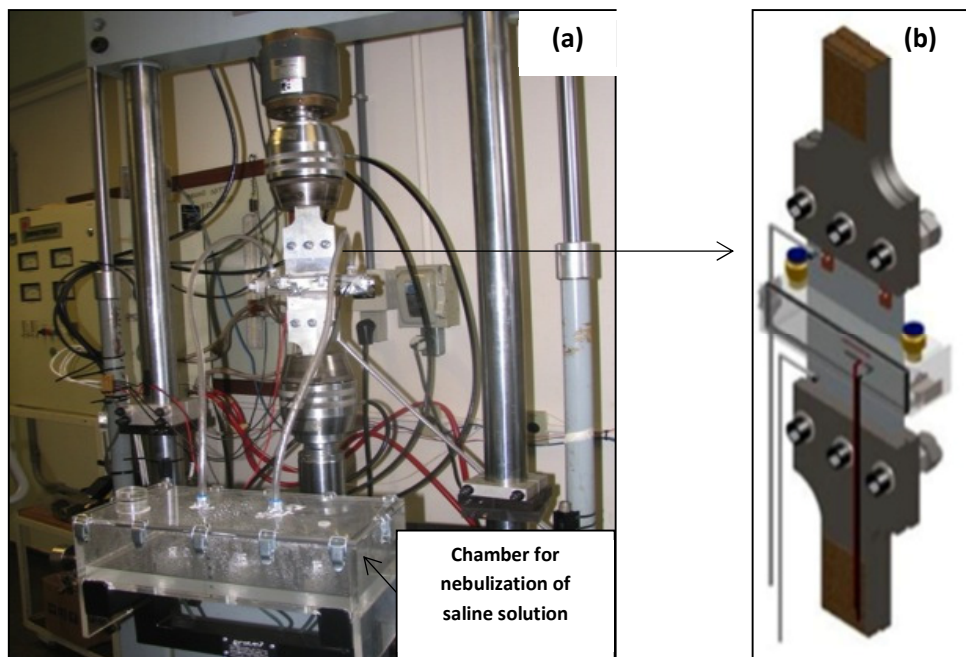


Figure 11 - Corrosion Fatigue Test (a) MTS Machine and (b) the Scheme of Crack Encapsulation System.

Figures 12(a) and 13(a) show the fatigue surfaces on tests under TWIST and FALSTAFF, respectively, for air. Both surfaces reveal striations that are inherent fatigue random loading. Figures 12(b) and 13(b) show the surface fracture at 3.5% NaCl, in these

surfaces, the striation is not clear and is possible to see oxides. Figure 12(c) shows marks made by corrosion products, the load pressed these products against the surface, as showed through the marks. Figure 13(c) does not show the marks of corrosion products.

The results of corrosion fatigue crack growth tests showed a competition between corrosion effects and load effects. The fatigue surfaces showed the presence of corrosion products that can promote closure induced by oxide.

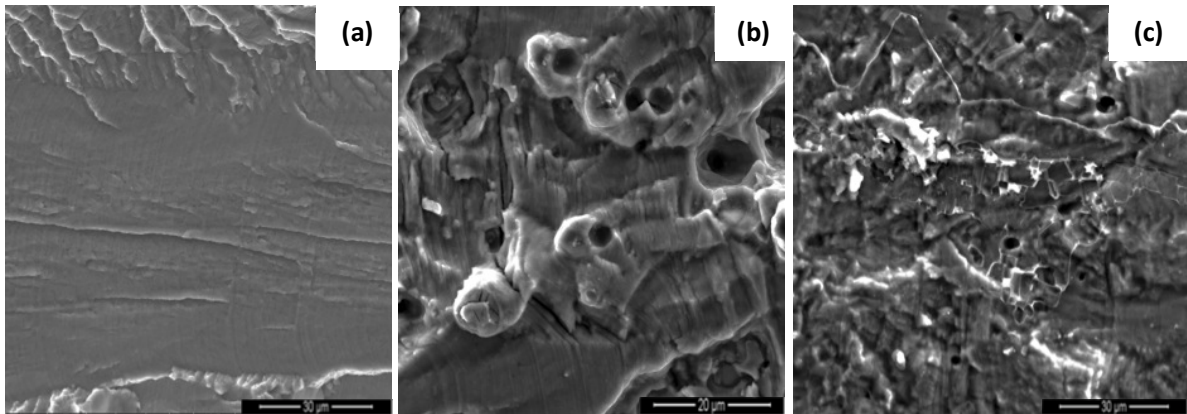


Figure 12 - Fatigue Fracture under TWIST Flight Sequence at (a) Air Environment, (b) 3.5% NaCl, (c) 5.0% NaCl.

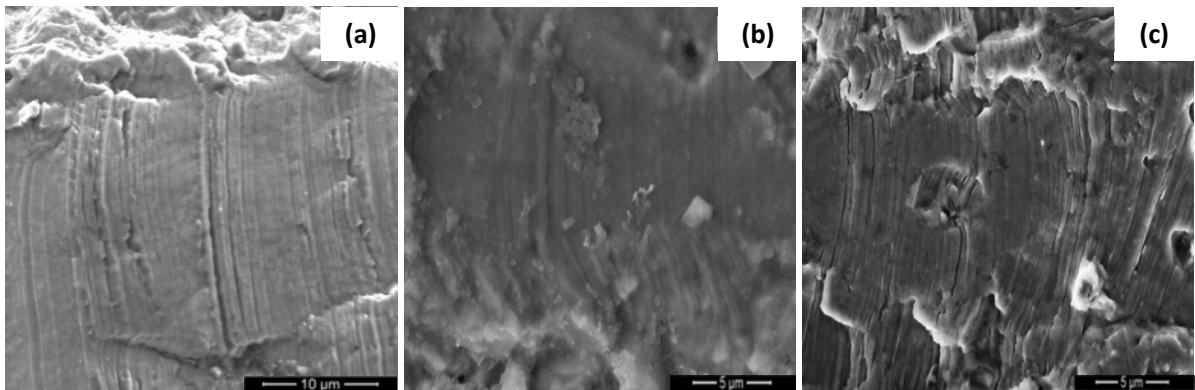


Figure 13 - Fatigue Fracture under FALSTAFF Flight Sequence at (a) Air Environment, (b) 3.5% NaCl, (c) 5.0% NaCl.

#### 4. METALLIC MATERIALS – STRUCTURES

During the period 2013-2015, there were important activities in Brazil related to structural testing, including tests of sub-components, components and full-scale fatigue tests, for different purposes such as compliance with certification requirements for existing aircraft, compliance with certification requirements for new type certificates, technological development and development of new aircraft.

In the last quarter of 2014, Legacy 500 (Embraer Project EMB-550) received its type certificate from Brazilian Aviation Agency (ANAC), from the Federal Aviation Administration (FAA) and from the European Aviation Safety Agency (EASA). Legacy 500 is a business jet powered with two Honeywell HTF7500 engines, with full fly-by-wire controls, maximum range of 3,125 nm and maximum operation altitude of 45,000 ft. Figure 14 shows the outline of this aircraft.

Most of the Legacy 500 structure is metallic, and all the necessary development and certification tests for its structure were performed between 2011 and 2014. The composite parts of its primary structure had dedicated test specimens that were subjected to static ultimate load tests, residual strength tests and fatigue tests (including the required knock-down factors and induced damages) prior to its type certification.

Its full-scale fatigue test was performed during the year of 2014, and due to a relatively short design life (i.e., for business applications), to a high efficient testing scheme and a small number of findings observed during the test, two lifetimes of the full-scale fatigue test were completed just after the first aircraft deliveries. Now the test specimen is being subjected to testing for a third lifetime for development purposes. Figure 15 shows an outline of the EMB-550 full-scale fatigue test.

The Legacy 500 wing lower skin panel consists of a set of machined plates connected by means of spanwise fastened splices in order to assure a multiple load path damage tolerant design. Despite the overall lower skin residual strength capability, the configuration of each skin plate was designed in order to “optimize” its crack propagation behavior. In the integrally stiffened panels, crack containment features, known as crenellations, were added to the existing blade stringers. The optimum configuration (i.e., the one that yields a minimum weight while assuring a maximum crack growth period) was tested against a conventional integrally stiffened panel. For this development, four stiffened panels (two with crenellations and two without) were subjected to spectrum loading, with two slightly different load magnitudes. Figure 16 shows the general view of the panel test device, and Figure 17 shows as an example the crack growth results for configurations 2 (without crenellations) and 4 (with crenellations). Although the initial half-notch size for all specimens was 4 mm, initially a constant amplitude loading was applied until the crack half-size reached 6 mm, and from a natural fatigue crack a variable amplitude loading was then applied.

Besides the direct comparison between measured crack growth results for both baseline and optimized configurations, both panel types were instrumented with strain gages and digital image correlation (DIC), from which a variety of strain information was obtained. From the crack growth results and from the DIC results, the Stress Intensity Factors could be successfully estimated through the experiments for increasing crack sizes. This work will be described with more details by Assunção and Chaves during the ICAF 2015 Symposium (Ref. [10]).

The full-scale fatigue tests for Embraer 170 (EMB-170) and Embraer 190 (EMB-190) were extended to three lifetimes, as means of supplying engineering data for compliance with Part 26 Subpart C Requirements. Both test specimens reached 240,000 pressurized flight cycles by 2014. Now the test specimens are being subjected to residual strength tests and teardown inspections. Figure 18 shows a general view of EMB-190 full-scale fatigue test specimen.

In terms of the application of new technologies in structures, during the last years a set of static and fatigue tests were performed for a configuration corresponding to a typical fuselage of a regional aircraft. A summary of these tests is presented in this review. A more detailed discussion about the barrel tests, their results and the technologies involved was presented during the AEROMAT Conference in 2014 (Ref. [11]).

Together with the existing riveted assemblies, panels joined and assembled via Friction Stir Welding (FSW), Structural Bonding and Fiber Metal Laminate (FML) were included in these demonstrators. FSW was applied to longitudinal and circumferential butt joints, skin-to-stringer connections and window frames. Bonding was applied to skin-to-stringer connections and to window frames. FML was applied to the door cutout area. The application of all these technologies led to a significant reduction in the number of fasteners and parts in the overall assembly, as expected.

While the static tests were performed for a set of limit and ultimate loading conditions (gusts, maneuvers, pressurization), the fatigue test specimen was subjected to a complex fuselage spectrum loading condition for a test period corresponding to three lifetimes of a typical regional aircraft, such as ERJ-145.

For the first two lifetimes the intact structure was tested in order to verify the structure durability. For the third lifetime many artificial damages were introduced and the crack propagation was monitored during the test progress, such that many crack growth scenarios could be evaluated in depth.

Figure 19 shows an overview of the barrel fatigue test specimen and rig.



Figure 14 – Legacy 500 (EMB-550) Executive Jet.



Figure 15 – Legacy 500 (EMB-550) Full-Scale Fatigue Test Overview.

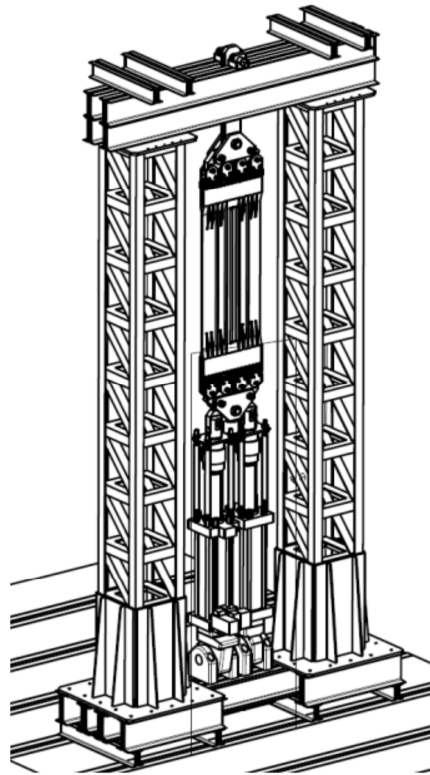


Figure 16 – Lower Skin Panel Crack Growth Test Device – General View.

**Comparison - Crack Propagation Behavior (Effect of Crenellations)**

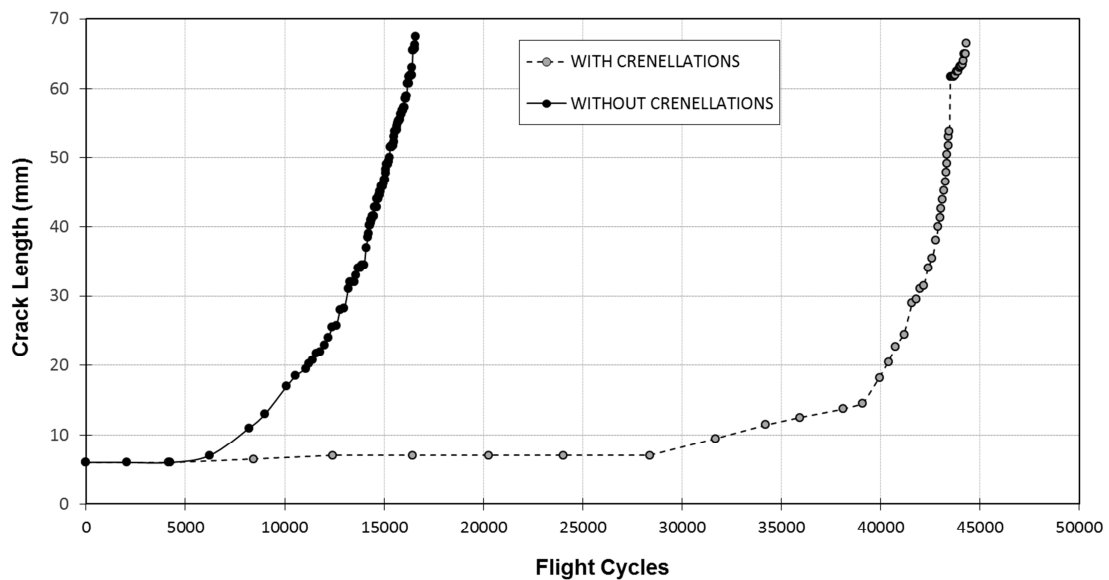


Figure 17 – Crack Growth Results for Skin Panel Specimens.

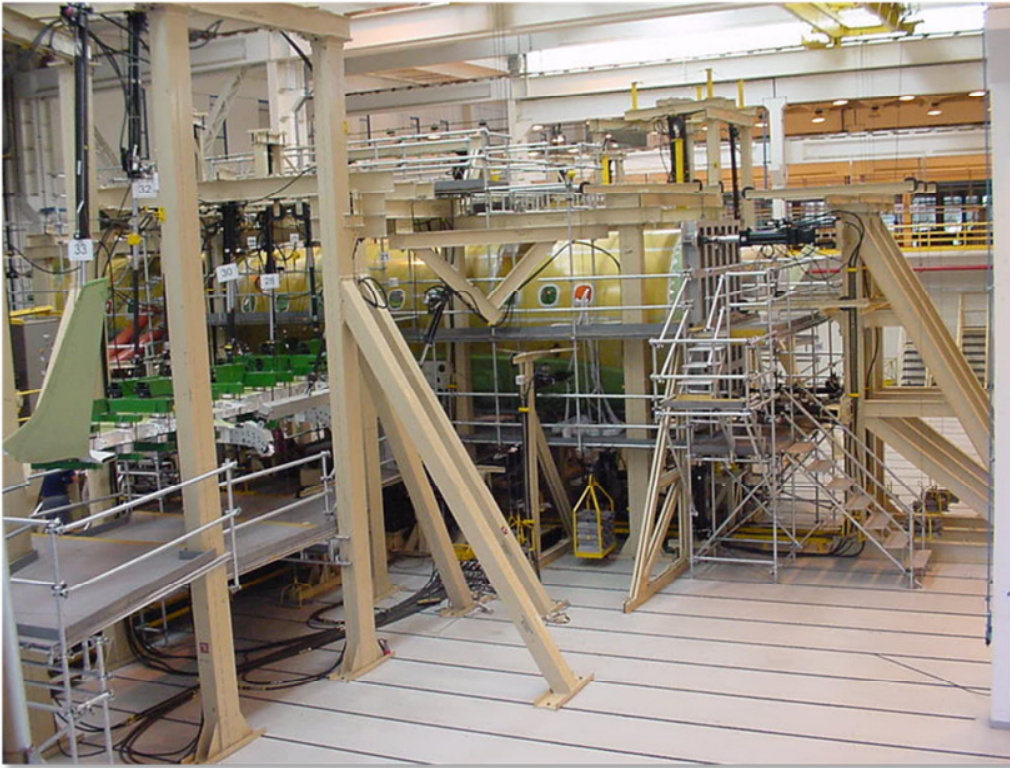


Figure 18 – ERJ-190 Full-Scale Fatigue Test Specimen.

Another concept under evaluation is an advanced wing spar with parts welded with FSW technology. The concept was presented by Aleris and Embraer during the AEROMAT Conference in 2014 (Ref. [12]). Some advantages of this concept are the reduction of weight by means of new alloys application with higher performance using the “design for concept”, as well as the possibility to reduce manufacturing costs. Figure 20 shows the parts comprising three different aluminium alloys successfully welded. The lower cap is made of extruded AA7181-T73511 that presents superior fracture toughness and fatigue crack growth properties when compared to most conventional aircraft aluminium alloys. This sub-component demonstrators will be later assembled to a wing structure and subjected to service-like conditions for verification of their fatigue and crack growth performance.



Figure 19 – Fuselage Barrel Fatigue Test Specimen and Rig.



Figure 20 - Advanced Wing Spar Concept.

## 5. COMPOSITE MATERIALS

An experimental study on the durability of stiffened composite panels with skin/stiffener initial flaws in the post-buckling regime (Ref. [13]) is part of the research of fatigue in composites being carried out by Professor M. Donadon and his team in the Aeronautical Institute of Technology (ITA).

The composite material skin-stiffener joints are increasingly using secondary bonding or co-curing to reduce weight and cost. This concept has the advantage of reducing the weight and cost of the part. However, the possible debonding of the stiffener in the post-buckling regime should be investigated particularly if a flaw in the adhesive layer between the skin and the stiffener exists. These defects may potentially degrade the joint interlaminar strength possibly inducing delamination.

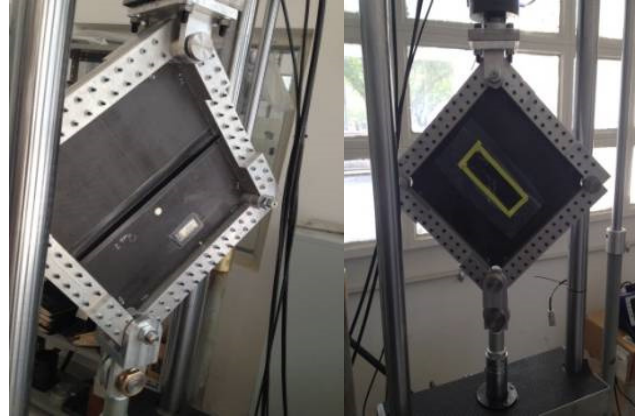
The work presents an experimental investigation on the mechanical behavior of composite skin/stiffener interface with an initial flaw under compressive and in-plane shear cycled loadings. The specimens were cyclic loaded in the post-buckling regime in order to investigate the fatigue damage tolerance of the panels. The specimens had an intentional flaw of 50 mm in the interface between the skin and the stiffener, located at the central region of the panels.

Figure 21 depicts the two panels and loading configurations evaluated.

The load levels used to test each panel configuration were based on finite element analyses. The finite element models accounted for geometrical and material non-linearities as well as interfacial and in-plane progressive failure modeling. The predicted buckling modes and buckling loads are shown in Figure 22. The cyclic tests were interrupted every 3,000 cycles for each panel configuration. After that, the panels were quasi-statically loaded in the post-buckling regime in order to investigate the effects of the cumulative skin/stiffener damage on the residual stiffness of the panels (see Figure 23). It becomes evident from Figure 23 that the structural responses of the tested panels were not significantly affected by the flaw size in the adhesive layer between the skin and the stiffener, within the load range studied in this work. Ultrasound inspections revealed a very low crack growth rate in both panels cycled up to 30,000 cycles.

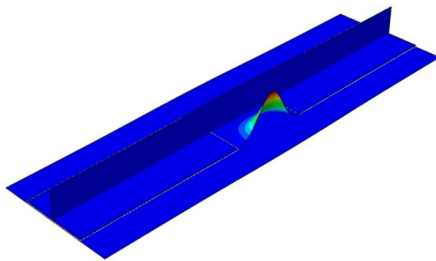


(a) Compression

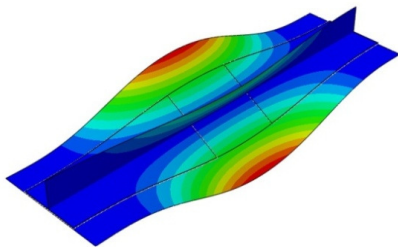


(b) Shear

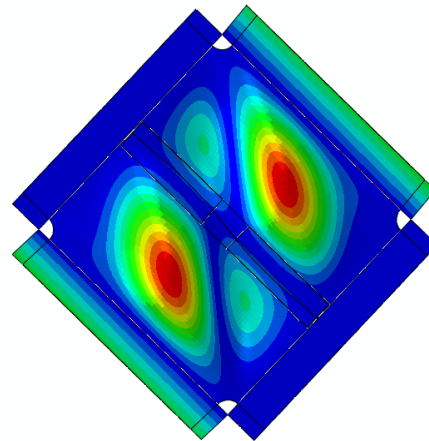
Figure 21 – Outline of Durability Test Setup.



(a) Local Buckling in Compression:  
 $P_c=12.8$  kN

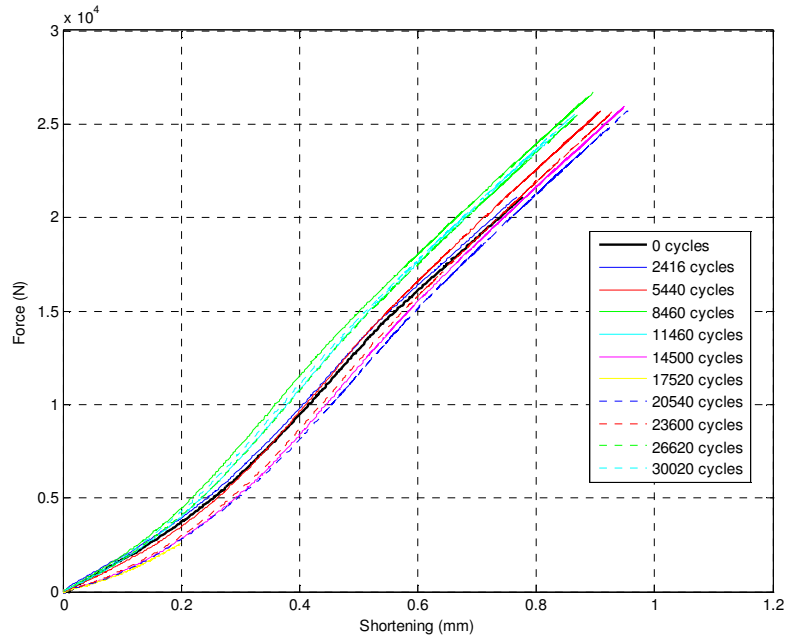


(b) Global Buckling in Compression:  
 $P_c=27.1$  kN

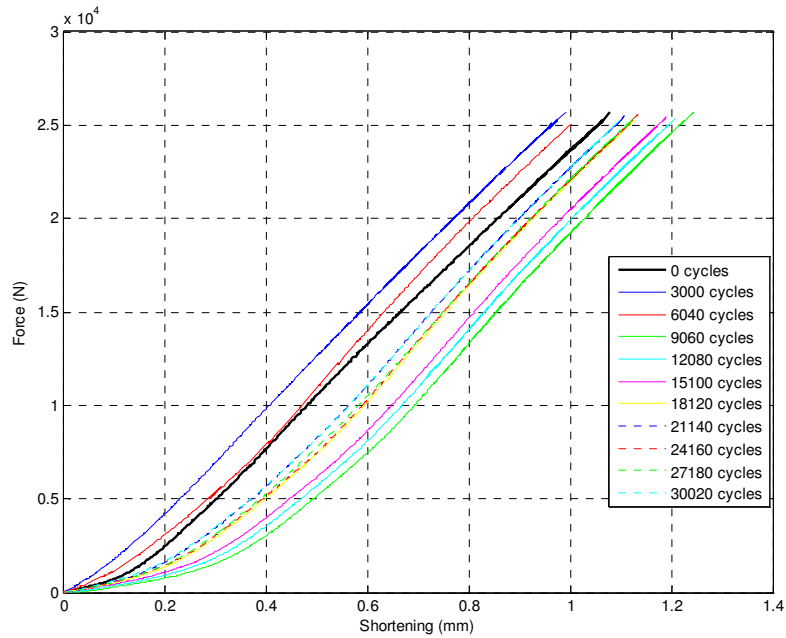


(c) Global Buckling in Shear:  $P_c=17$  kN

Figure 22 – Predicted Buckling Loads/Mode Shapes.



Load vs. Displacement – Compression Loading



Load vs. Displacement – Shear Loading

Figure 23 - Load vs. Displacement Curves Obtained from the Durability Tests.

Another study from B. Endo, M. Donadon and co-workers addresses the characterization of interlaminar fracture toughness of a carbon fiber-epoxy material with thermo-mechanical effects (Ref. [14]). Their paper presents the procedures used and the results of an experimental study performed to obtain the values of interlaminar fracture toughness ( $G$ ) of a laminate using  $0^\circ$  carbon-epoxy prepreg fabric plies and manufactured via HLUP under three different temperatures. Double Cantilever Beam (DCB) tests were performed to evaluate mode I toughness at  $-54^\circ\text{C}$ ,  $25^\circ\text{C}$  and  $80^\circ\text{C}$ . The tests have followed procedures described in the standard ASTM D5528-01; the data were collected and analyzed using a routine developed in Matlab®. Finally the temperature influence on the interlaminar fracture toughness mode I was assessed.

The interlaminar fracture toughness for Mode I ( $G_I$ ) is given by:

$$G_I = \frac{3P\delta}{2b(a + |\Delta|)}$$

Where  $P$  = load,  $\delta$  = displacement,  $b$  = specimen width and  $a$  = delamination length.  $\Delta$  is a correction for  $a$  that becomes necessary for a DCB specimen, and can be obtained experimentally through a linear graph of the cubic root of flexibility depending on the delamination length.

Figure 24 shows the geometry of all specimens tested, while Figure 25 shows  $G_I$  values of all the specimens tested at  $25^\circ\text{C}$ . Table 2 summarizes  $G_I$  average values found from the tests under the three temperature conditions. It is possible to observe that  $G_I$  increases with the increase of the temperature, and from  $-54^\circ\text{C}$  to  $25^\circ\text{C}$  the differences reach up to 36%.

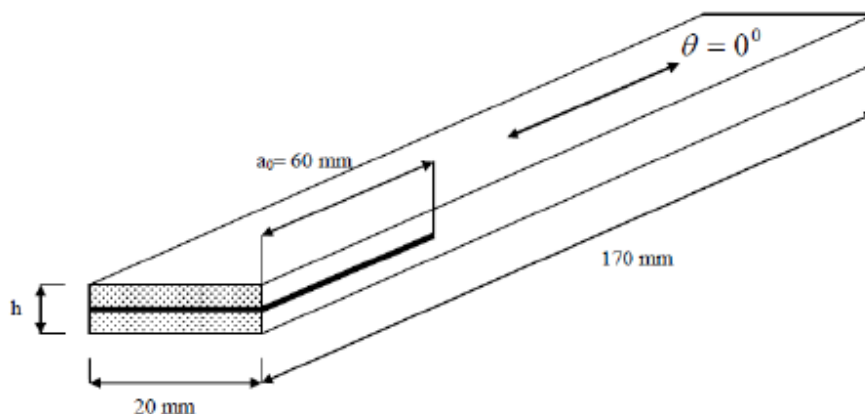


Figure 24 - Dimensions of DCB Specimens used for Interlaminar Fracture in Mode I Characterization ( $h = 3.04$  mm).

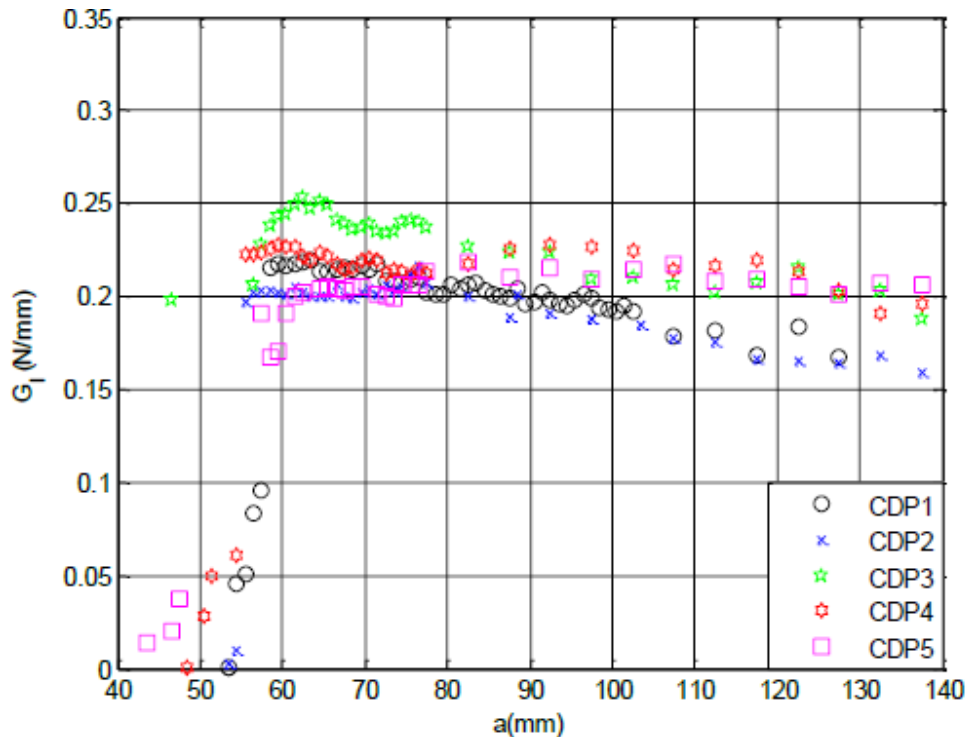


Figure 25 - Curve  $G_I$  Versus Delamination Extension for Specimens Tested at 25°C.

Table 2 - DCB Test Results Comparison Under Different Temperatures.

DCB test temperature	$G_I$ average (N/mm)	$G_I$ standard deviation (N/mm)
-54°C	0.1448	0.0284
25°C	0.1977	0.0177
80°C	0.2370	0.0276

Another work from R. Sales, M. Donadon and co-workers (Ref. [15]) shows a comparative study of Mixed Mode I+II interlaminar fracture toughness of reinforced carbon laminates manufactured by VaRTM and HLUP. The main objective of this research work is to investigate and compare the Mixed-mode interlaminar fracture behavior of carbon composite manufactured by VaRTM and HLUP and subjected to stresses at high temperatures. High temperature Mixed-mode Bending (MMB) tests were performed at 80°C. Different mode ratios were tested ( $G_I/G_{II} = 25\%$ ,  $G_I/G_{II} = 50\%$  and  $G_I/G_{II} = 75\%$ ) for each manufacturing process. The experimental results were correlated and conclusions were drawn.

The loading configuration to this test is MMB type, as shown in Fig. 26. Different mode ratio  $G_{Ic} / G_{IIc}$  are obtained changing the distance  $c_a$ .

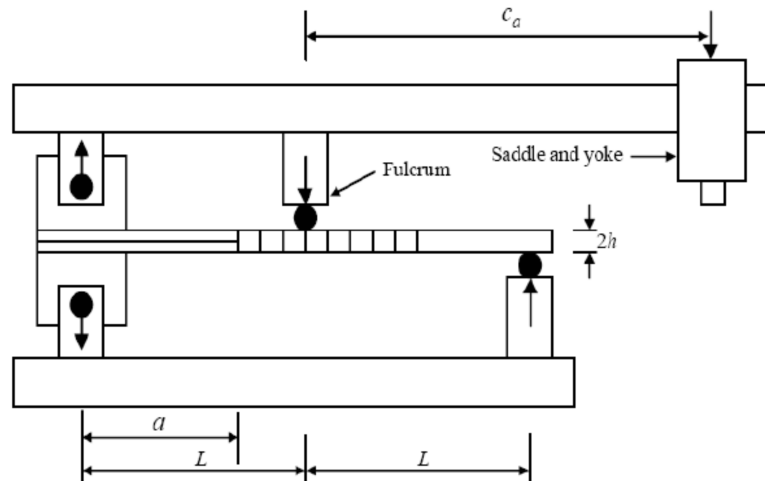


Figure 26 - Loading Configuration for DCB Testing under Mixed Mode I/II.

In VaRTM specimens, it was noticed that  $G_I$  and  $G_{II}$  values are higher than in HLUP specimens due to the influence of the resin system. The resin system used in HLUP specimens has lower fracture toughness values. This aspect promotes a brittle behavior decreasing the interlaminar mechanical strength.

Another study from M. Shiino, M. Donadon and co-workers (Ref. [16]) refers to the applicability of standard delamination tests (double cantilever beam and end notch flexure) for 5HS fabric-reinforced composites in weft-dominated surface. This study explores delamination tests in woven composites. A 5HS carbon/epoxy composite with a weft-dominated surface is evaluated. Tests were conducted in double cantilever beam and end notch flexure configurations using an energy-based approach for data reduction in Modes I and II, respectively. The results were assessed in terms of delamination resistance curves ( $R$ -curves). Both delamination modes showed consistent behavior for extending the application of the standard procedures, as the energy variation can describe well the crack growth dependence of the irregular surface caused by the crimp, which was more pronounced for mode I.

In another study from M. Donadon and D. Lauda (Ref. [17]), a continuum damage mechanics failure model to predict mixed-mode delamination growth in composite laminates subjected to static and high-cycle fatigue loading is proposed.

The proposed formulation has been developed for robust nonlinear finite element formulations based on explicit direct time integration schemes, particularly the central difference method. The failure model has been implemented as a user-defined material

model into ABAQUS/Explicit© finite element code within C3D8 hexahedron solid elements. Numerical simulations were performed at coupon level for double cantilever beam, end-notched-flexure, mixed-mode bending and mixed-mode flexure specimens.

Numerical predictions obtained using the proposed constitutive models were compared with experimental results available in the open literature for DCB, 4ENF, MMB and MMF coupons. A very good correlation between numerical predictions obtained using the proposed damage model and experimental results was found in terms of damage initiation and damage propagation typical coupons subjected to static and fatigue loading conditions.

The proposed damage model seems to be a robust and reliable design tool that enables the prediction of static and fatigue-driven delamination in composite aerostructures. It can also be easily combined with an in-plane damage model enabling prediction of in-plane failure modes such as matrix cracking, fibre failure either in tension or compression and in-plane shear failure.

Finally, a study from Dr. A. Ancelotti and co-workers (Ref. [18]), from Federal University of Itajubá (UNIFEI) proposes a methodology to obtain the carbon fiber/epoxy composite limit strain for structures surviving 120,000 cycles, that is typically twice the design life of a regional aircraft. In this work, the damage progression was evaluated using stiffness reduction and hysteresis loop analysis in order to obtain dynamic and secant modulus.

Figure 27 presents a flowchart of the methodology used to determine limit strain. During each test, the specimen is initially pre-loaded to about 50% of ultimate tensile strength. This procedure eliminates involuntary movement of the extensometer and avoids any loss of reference due to the eventual rupture of misaligned carbon fibers in the specimens. Previous studies have determined that a pre-load of 50% of ultimate tensile will not have any influence on the fatigue life.

According to the flowchart, the specimen is loaded to a prescribed strain level and then submitted to fatigue cycling. If the specimen fails, the number of cycles is recorded and the next specimen is tested at a different maximum strain level. If the specimen survives after 120,000 cycles (two aircraft lifetimes), a residual strength test is performed and the factor relating the residual tensile strength, after cycling fatigue, and the ultimate tensile strength, reduced statistically to a B-basis value, is calculated. This (residual strength / ultimate strength) relation is named RF (Ratio Factor). A RF greater than 1 means that residual tensile strength is higher than the B-basis value. Consequently, the strain level applied to the next specimen must be increased. Conversely, if the residual tensile strength is lower than the B-basis value, the strain applied for the next specimen must be decreased. The limit strain corresponds to the point where the RF factor is approximately equal to 1.

The fatigue limit strain observed for the prepreg composite material evaluated for this study was around 8300 to 8700 $\mu\epsilon$ . This demonstrated the possibility of increasing the typical load level applied to composite structures which is normally in the vicinity of 4000 $\mu\epsilon$ .

Despite limited data points, the *S-N* curves generated in this work show that the stress limit is around 80% of the normalized ultimate tensile stress level. Hysteresis curves generated from modulus tests conducted at discrete intervals during the fatigue tests, revealed a stiffness reduction of 5% for dynamic and secant moduli. It was determined that hysteresis measurements, acquired during fatigue tests within the limit strain, provide a reliable method for quantifying damage accumulated from fatigue of composite materials. The proposed methodology may be used as a basis for determining material design allowables when fatigue is a critical issue.

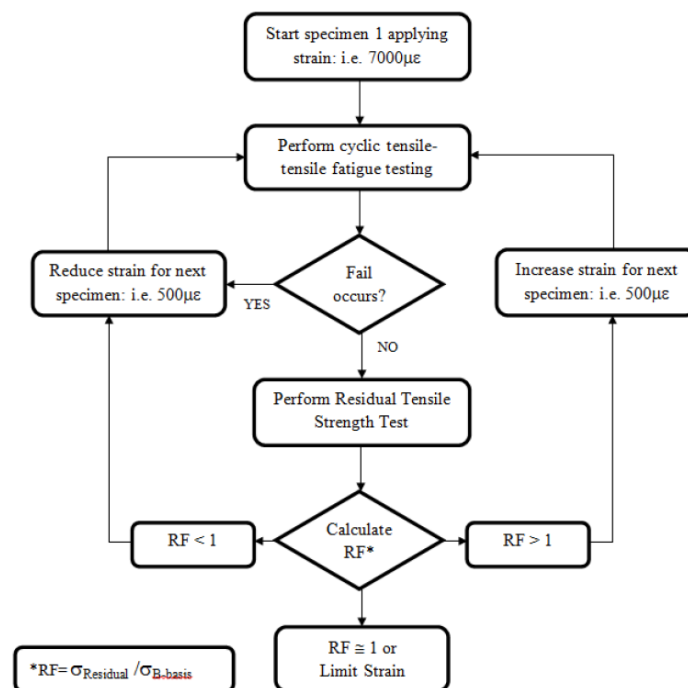


Figure 27 - Flowchart for Fatigue Limit Strain Determination.

## 6. BONDING

Regarding fatigue of bonded joints, a Ph.D. Thesis of C. Souza (Ref.[19]), from University of Campinas (UNICAMP) finished in 2013, brought interesting information on applications, and will be discussed in the present review.

The design of bonded joints is predominantly based on stress analysis as well as on the evaluation of displacement fields along the joint. In the case of cyclic loading, or fatigue, it is also necessary to develop models to predict the fatigue life of cracks in the adhesive layer and adherends.

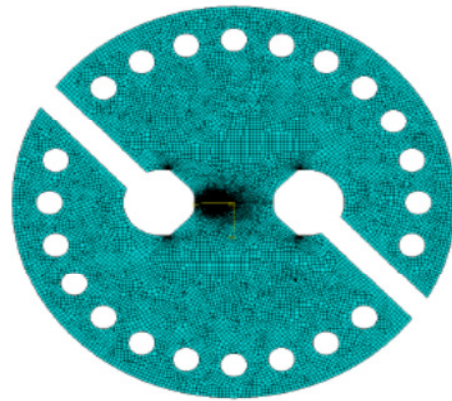
The main objective of Souza`s work was to study the behavior of bonded joints in metallic aircraft structures under fatigue loading, through analytical models, numerical models and

experiments. During this work, static, fatigue and fracture toughness tests were carried out. subcomponents that represent real aircraft structures were also designed and tested. The joints were modeled using commercial finite element software ABAQUS®. An analytical model to predict the fatigue life of bonded joints based on the formulation of Krenk (1992) and the Paris-like Law was also developed and implemented. Finally, a technique to measure the fatigue crack growth during a test automatically, i.e., without stopping the test to make visual measurements was developed.

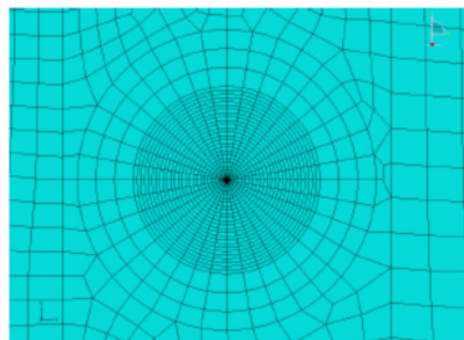
Among other tests, in order to obtain the Energy Release Rate for Mode I, Mode II and Mixed Mode (Mode I+II), the Arcan specimen was used. Figure 28(a) shows the overview of the testing machine. Figure 28(b) presents the outline of the FEM model used for comparison and 28(c) shows the mesh refinement in the crack tip region. The plot in Figure 29 shows the relationship between  $G_I$  and  $G_{II}$  for a mixed mode case, where experimental and analytical results were compared. A similar level of correlation was observed also for Mode I and Mode II cases.



(a)



(b)



(c)

Figure 28 – Arcan Tests and Simulation.

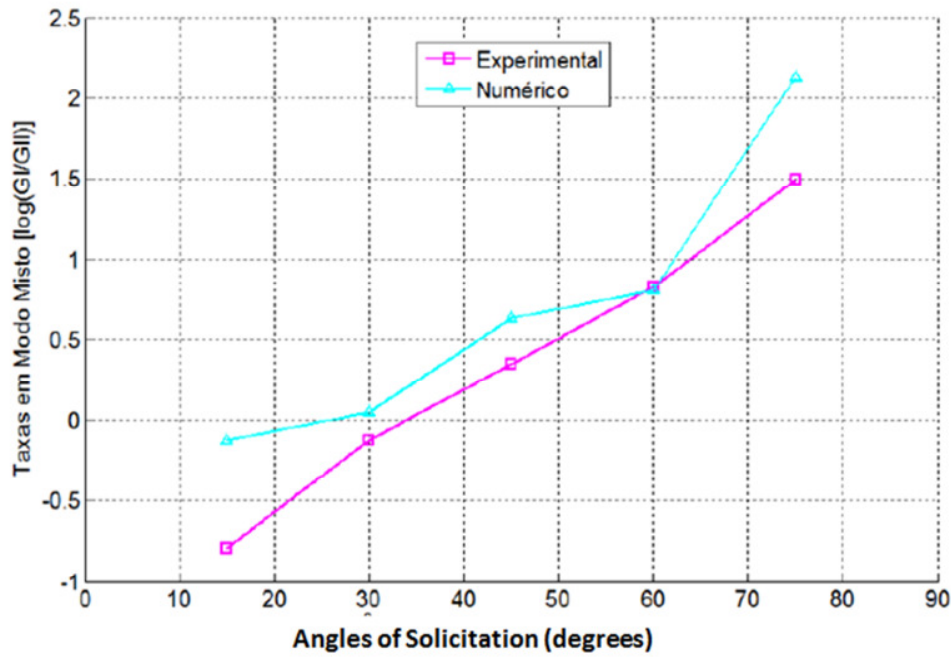


Figure 29 – Comparison Between Tests and Numerical Simulation – Mixed Mode.

From the aircraft applications point of view, panels with bonded repairs were tested, as shown in Figure 30. The crack size was monitored visually and with via ultra-sound, with strain levels during the test were measured via strain gages.

Figure 31 shows some details of the numerical analysis performed with ABAQUS® for this specimen, and Figure 32 shows the comparison between experimental and numerical results in terms of crack propagation (crack length in millimeters vs. number of cycles).

As a general conclusion from this work, an analytical model was developed and implemented in a tool that works integrated with ABAQUS®, and this model was validated by means of various experiments. Other tests with compact and DCB specimens, although not presented here, were also performed and the model showed good agreement for these configurations as well.

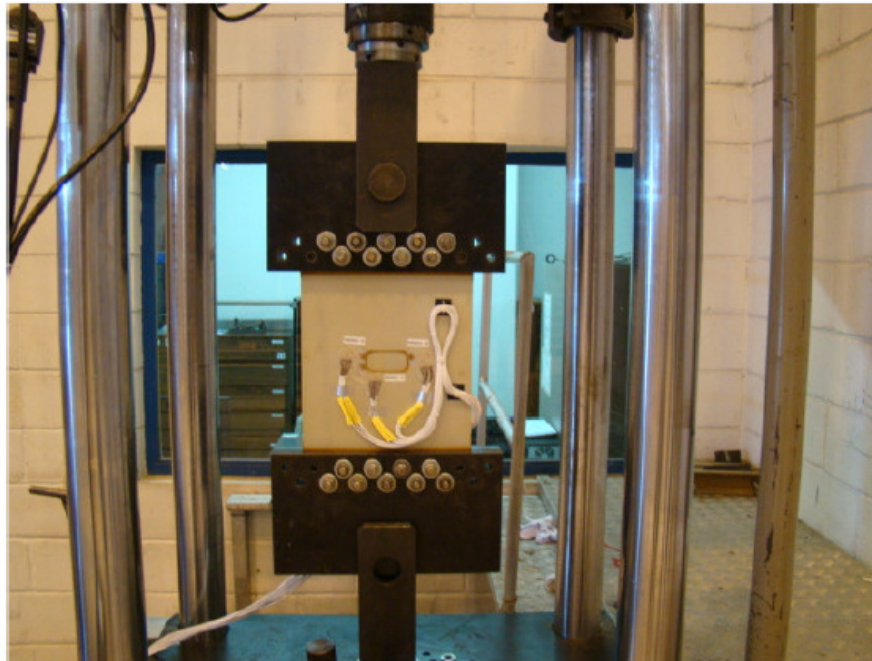


Figure 30 – Bonded Repair - Test.

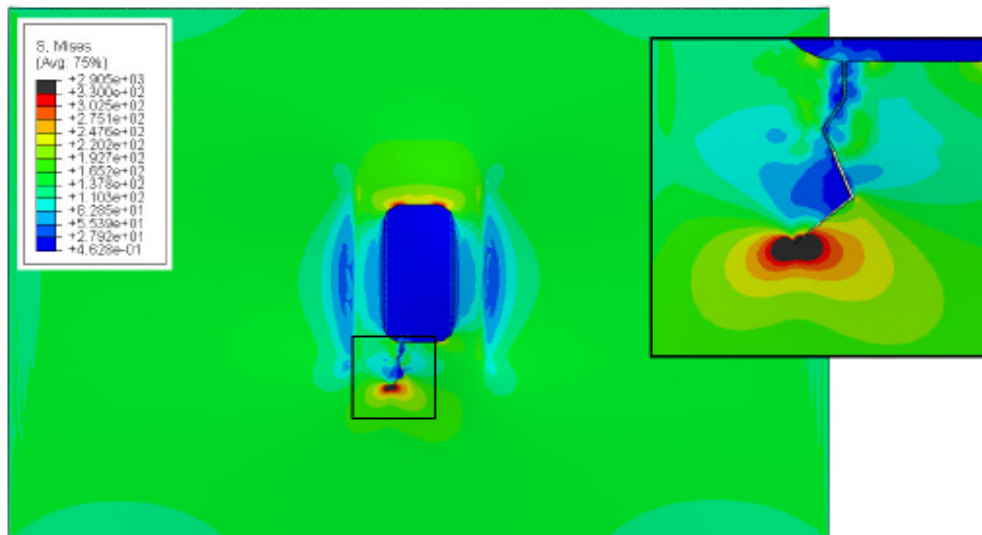


Figure 31 – Bonded Repair - Numerical Analysis.

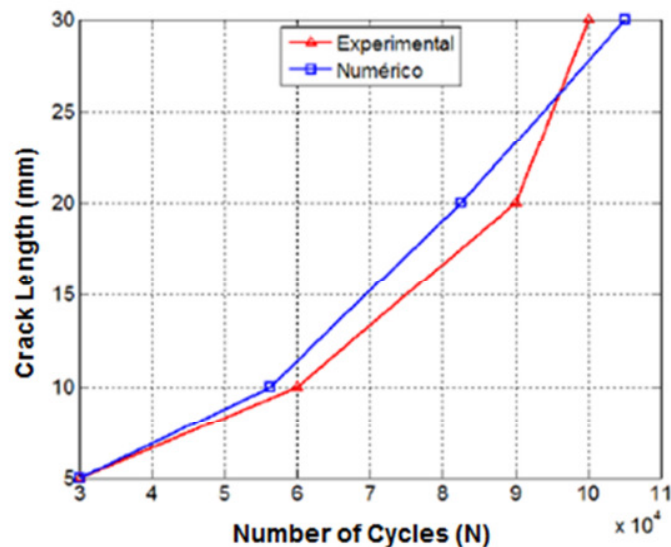


Figure 32 – Bonded Repair Crack Growth – Experimental vs. Numerical Results.

A more conceptual work on bonding of metallic materials developed in cooperation with the Deft University of Technology (Ref. [20]), resulting in the Ph.D. Thesis of Captain D. Bürger, from the Brazilian Air Force, will be presented in this review. Part of his work was presented in the 33<sup>rd</sup> ICAF Conference, in 2013 (Ref. [21]).

Adhesive bonding is a joining technique that offers potential for improvement in the fatigue behavior of a structure, resulting in reduced weight. However, predicting the fatigue behavior of a bonded joint for its use in a damage tolerance design philosophy still remains a problem with no satisfactory solution. Often, the joint is subjected to a combination of peeling and shearing stresses. Hence, one of the most important factors influencing the fatigue behavior of an adhesively bonded joint is the Mode Ratio.

The objective of Dr. Bürger investigation was to study of the Mode Ratio on the fatigue behavior of a bonded joint. First, the fatigue disbond mechanisms were investigated throughout the entire Mode Ratio range and compared to fatigue delamination mechanisms.

After the mechanisms were identified, a parameter related to the mechanisms was chosen as similitude in the Paris relation and the Mixed-Mode fatigue disbond model was developed. Later, the model was evaluated on a different adhesive and on a condition of variable Mode Ratio. The fatigue disbond mechanisms study identified the local principal stress as the driving force for the micro-crack formation and growth, and the Mode Ratio was identified as the controlling parameter for coalescence between the micro-cracks. Based on these findings, a parameter directly related to the principal stress was proposed as a similitude parameter.

Additionally, a linear interpolation between Mode I and Mode II parameters of the Paris relation was proposed to predict the Mixed-Mode fatigue behavior.

Thus, the model predicts the fatigue behavior for the entire Mode Ratio range using only pure Mode I and pure Mode II as inputs. The evaluation of this model revealed that it presents good predictions for Mode Ratios in the range of 0% to 50% and conservative predictions in the range of 50% to 100%. The model also seems to be valid in a variable Mode Ratio condition.

The limitations and shortcomings of the model along with the limitations of using a damage tolerance philosophy on adhesive bonding were discussed. Despite these issues, the model is an improvement over the models available in the literature because it captures some of the phenomena involved in the Mixed-Mode fatigue disbond.

Additionally, the model also reduces the amount of empirical data required for its implementation.

The following are some important results from Dr. Bürger work.

Figures 33 and 34 show experimental results in terms of fatigue disbond growth for Mode I, Mode II and Mixed Mode (Mode I+II) for load ratios 25%, 50% and 75%. Figure 35 presents the same data compared with the prediction from the model proposed by Bürger.

Figure 36 shows schematically the test specimens used for verification of disbond growth in single lap joints. Then Figure 37 shows the crack growth rates obtained from these tests, and Figure 38 presents the comparison between experimental results and the prediction from the model proposed by D. Bürger, when implemented in a FEM model in ABAQUS®. One additional curve corresponding to the Hart-Smith (HS) model is included in each plot, for comparison.

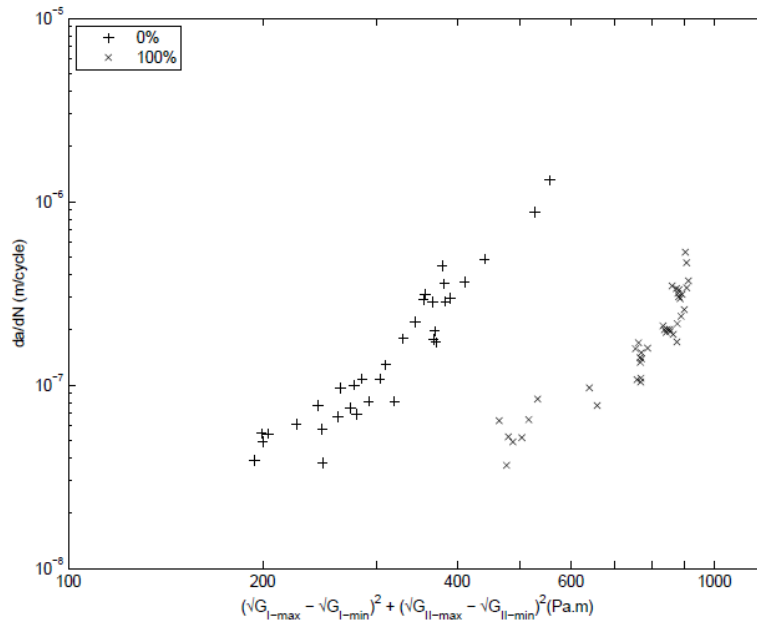


Figure 33 – Fatigue Disbond Growth Behavior. Pure Mode I and II.

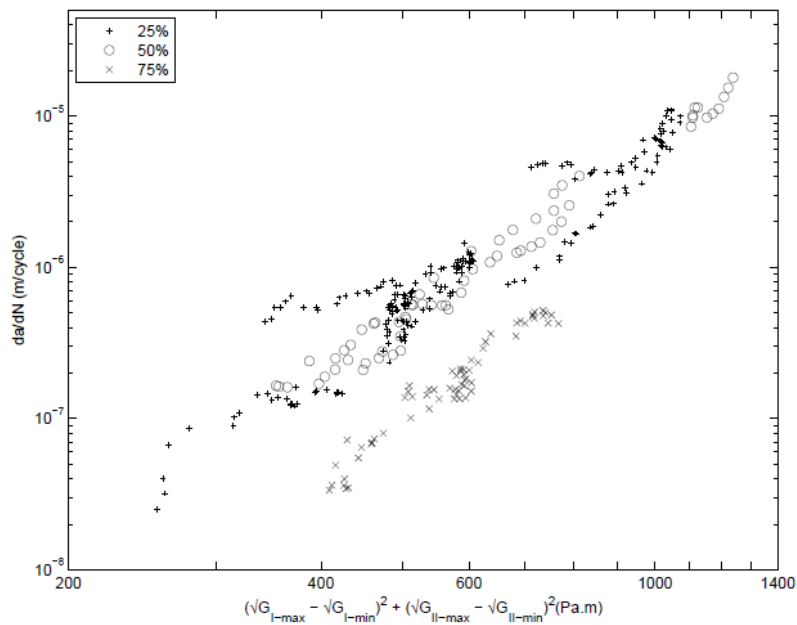


Figure 34 – Fatigue Disbond Growth Behavior. Mixed-Mode - FCG.

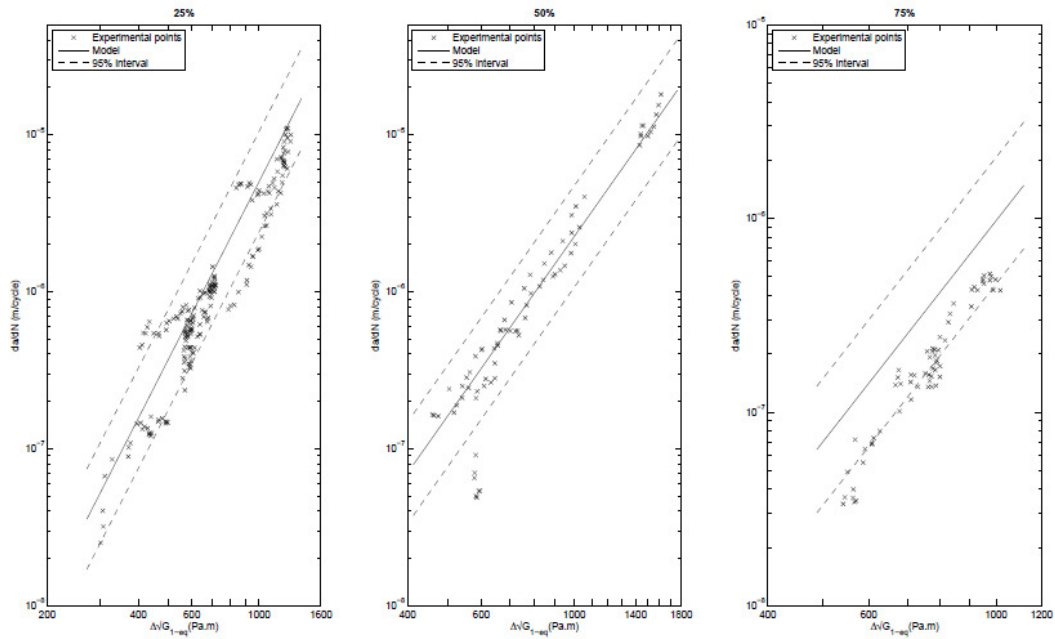


Figure 35 – Model predictions for the MM - FCG set of data.

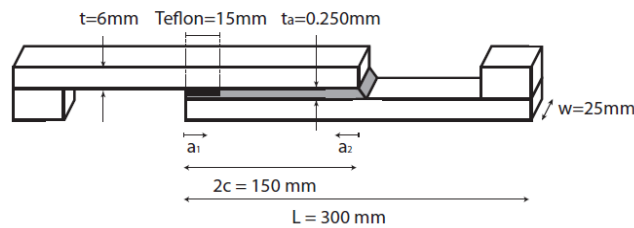


Figure 36 – Single Lap Joints - Specimen Details.

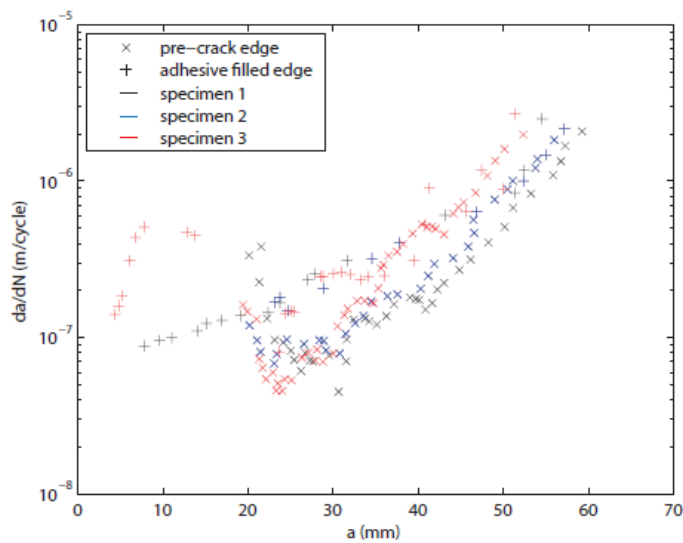


Figure 37 – Fatigue Disbond Growth Rate Results.

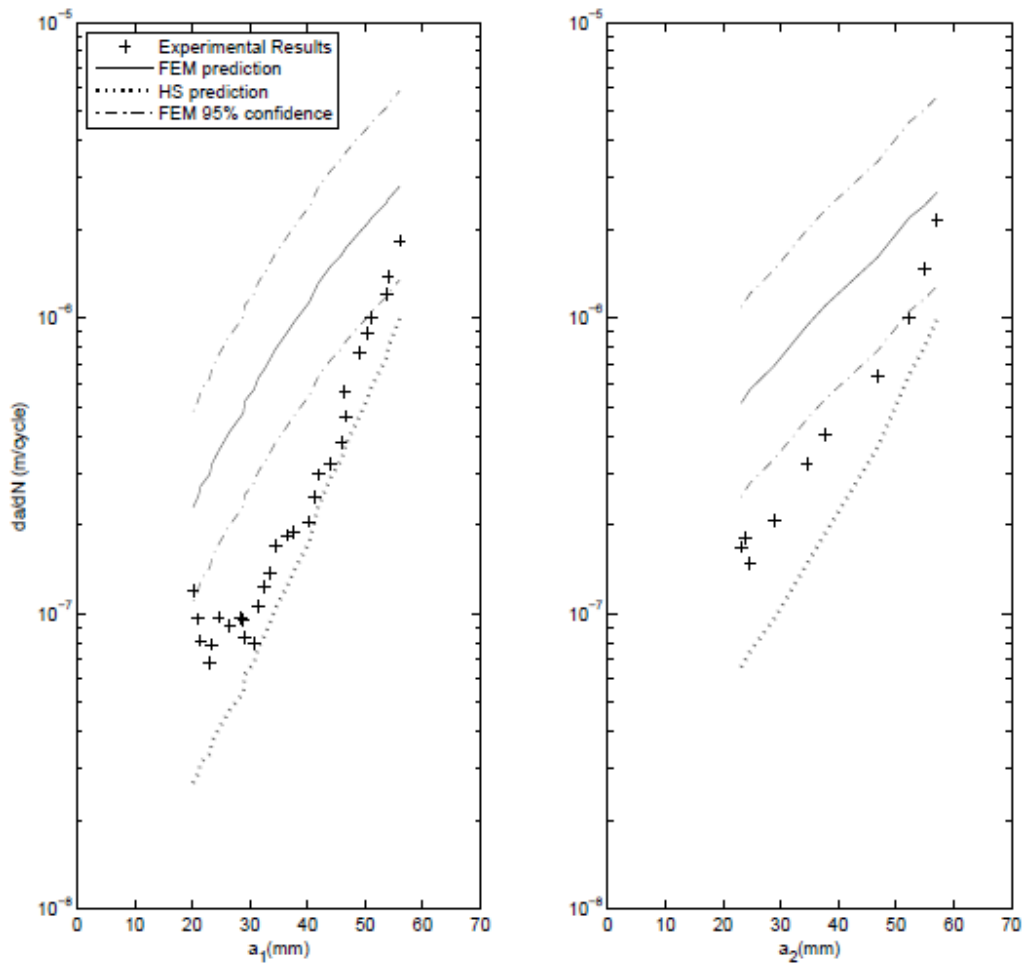


Figure 38 – FDG Prediction for Both Disbond Tips of a SLJ.

## 7. STRUCTURAL HEALTH MONITORING

Four works related to inspections and Structural Health Monitoring (SHM) will be discussed along this report.

The first work, by F. Dotta and L. Ceresetti (Ref. [22]), refers to the application of Lamb Waves technique to detect simulated damage in an orthogonal plane of the sensor network surface for corrosion detection application. The work demonstrates the evaluation of the Lamb Waves approach in order to detect and locate simulated damages in aluminium alloys placed orthogonally from the sensor network surface. The tests discussed in the work were performed using a typical aeronautical specimen configuration and Direct Image Path from Acellent Technologies. The experimental results indicate the

Lamb Waves technique is highly accurate and it has become promising application to detect corrosion damage. This study is part of a set study of several SHM Technologies, like CVM (Comparative Vacuum Monitoring), EMI (Electro-Mechanical Impedance), AE (Acoustic Emission), LW (Lamb Waves). Those studies are under Embraer's R&D program.

For the study, two rectangular aluminium specimens with a single fastened stringer was taken. The plate were made of alloy AA 2024 with 323mm x 223mm and 1.6mm of thickness, the stringer was made of AA 7050 from a standard extrusion profile and the rivet are aeronautical standard. Both specimens were monitored with Acellet's 1/4" circular PZT (Single SmartLayer). Figure 39 shows the manufactured specimens with PZT bonded. For each damage position a range of damage sizes was used: on the plate (sensor on stringer) 3 damage sizes were applied (0.5", 1.0" and 1.5" of diameter) and on the stringer (sensors on the plate) 2 damage sizes (0.5"and 1.0") were applied. These ranges of damage sizes represent, qualitatively, different levels of corrosion and improve the understanding of the threshold of the Lamb waves sensitivity for thickness reduction detection.

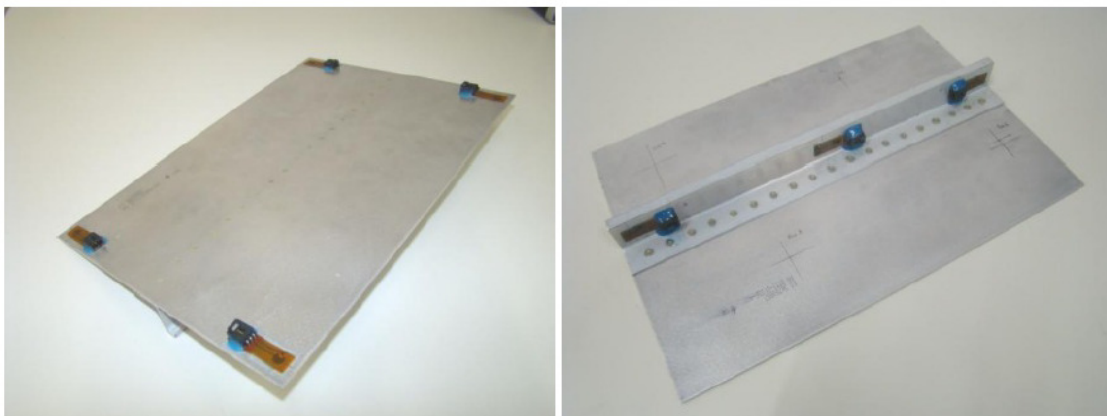


Figure 39 – Specimens 01 and 02 with PZTs Bonded.

Figure 40 shows the spectrograms of 200kHz of the damage detection using direct image path obtained thru Acellet's system. These spectrograms do not predict the damage size or location, but only representing the signal pattern change between the baseline and damaged specimen. The spectrograms shown change on the acoustic response on the structures with damage simulator in the orthogonal plane from the sensors.

Figure 41 shows the signal responses of the most affected path (higher scatter) for the sensors networks 3 and 4 at 200kHz. The black line is the baseline signal and the red line is the signal scatter. These plots show small changes in the signal in comparison with the baseline. It is enough to perform a corrosion assessment with low density sensor network on these laboratory specimens. Also, in this study the damage was simulated by the "sticky patches" and those approaches provide conservative results because the changes

on the acoustic response caused by the damage simulator are smoother than the real damage.

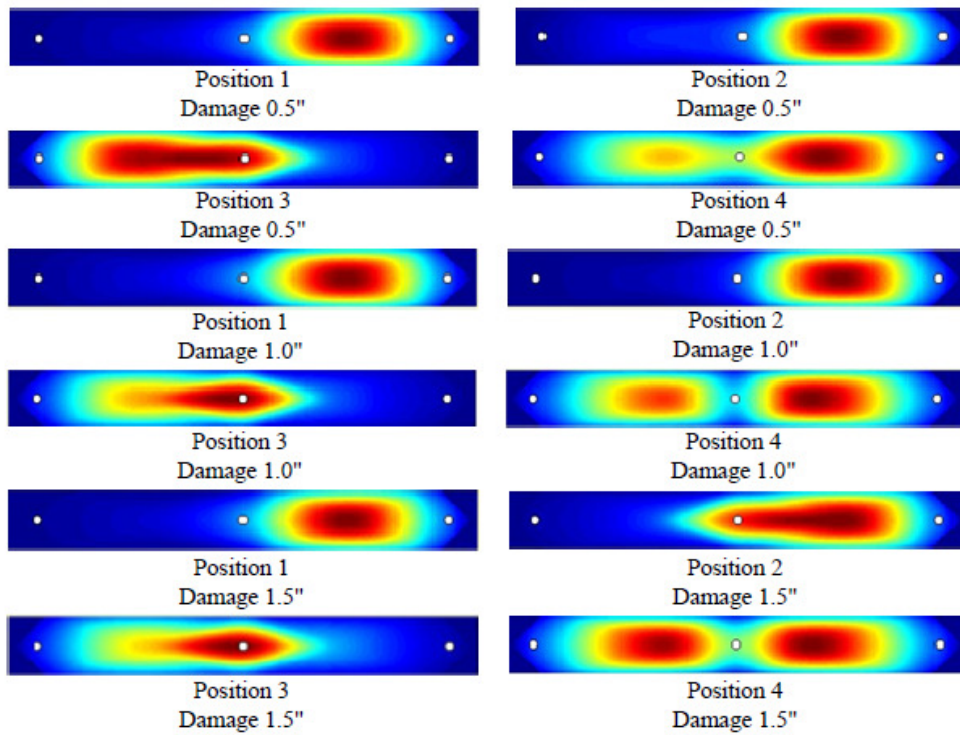


Figure 40 – Damage Identification Spectrogram at 200kHz Using Direct Image Path with Damage Simulator Positioned on the Plate and Sensor Positioned on the Stringer.

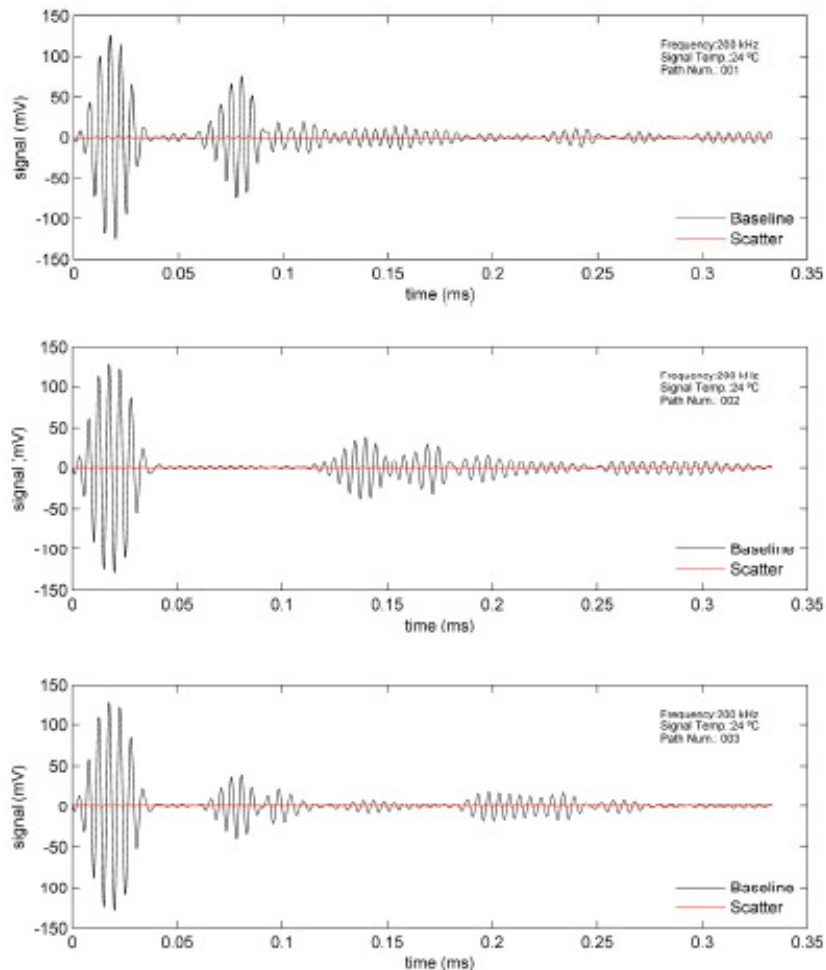


Figure 41 – Example of Signal Response of the Sensor Network with 3 PZT Positioned on the Stringer with Higher Scatter at 200kHz.

These results show changes in the frequency response (acoustic response) of the tested specimens, consequently representing changes of configuration, in this case a damage simulator (damper effect). The experimentation setup of this study provided conservative results because the "sticky patches" basically cause only a small damping effect on the signals. Real thickness reduction will cause a larger changes, and consequently, a larger scatter on the signals. The results presented here indicated the Lamb waves approach for corrosion detection when the sensor are in a orthogonal plane from damage plane is a viable detection method.

In another work from R. Rulli, F. Dotta and P. A. Silva (Ref. [23]), the authors present a visibility of full-scale fatigue tests and flight tests performed by Embraer including SHM systems.

Considered as promising technologies for monitoring structural parts, sensors networks including cables and connectors of CVM and LW were installed in an Embraer-190 aircraft. The two technologies have been investigated by Embraer within the company's effort on Structural Health Monitoring.

The tests performed with CVM and LW components (sensors, connectors and cables) installed in a flight tests aircraft focus on the investigation of the technologies' capabilities of withstanding the real aircraft operational conditions.

Periodic monitoring of these on-board sensors has been performed using CVM and LW ground equipments. Preliminary results on both partially and totally on-board equipments indicate that they can withstand the environmental and operational conditions; however, further tests need to be performed. Performing periodic inspections on ground with SHM systems lead to different qualification requirements when compared to those required for a complete on-board system that performs continuous monitoring. An overview of those two aspects of qualification requirements is also presented in the work.

*Ground Tests with CVM Technology:* Embraer has developed a project regarding study and evaluation of Comparative Vacuum Monitoring systems on ground.

Due to the technology characteristics and its relatively simple concept, the company has performed laboratory tests with CVM applying the technology in a metallic barrel test article and in the E-Jets Full-Scale Fatigue Test.

CVM sensors were applied to the continuous monitoring of a Metallic Barrel test. Cracks were detected starting with 2mm in length (loaded condition) or 3mm in length (unloaded condition) from the rivet head (for example, Figure 42). In addition to the metallic barrel test, Embraer installed around 260 CVM sensors in the Full-Scale Fatigue Test (FSFT) of the E-Jets aircrafts (Figure 43). Various regions and components have been subjected to periodic monitoring actions using this technology.

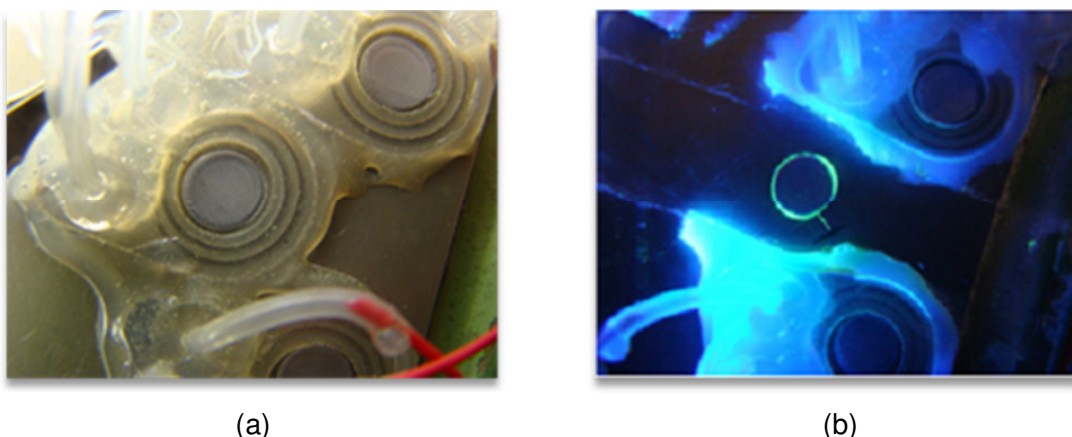


Figure 42 – Example of a Crack Detected by a CVM Sensor in the Metallic Barrel Test. (a) CVM Sensors Installed Around Rivets; (b) Sensors Removed and Dye Penetrant Testing Confirmed Presence of a 2mm Crack.



Figure 43 – CVM Sensors Installed in Various Regions of the E-Jets Full-Scale Fatigue Tests.

*Ground Tests with Lamb Waves Technology:* In addition, LW sensors were installed in the E-Jets FSFT and in the barrel test article. Various regions have been periodically inspected using LW system. The focus of these tests is to provide bulk information about LW sensors and systems, in order to evaluate their capabilities, installation, operation and maintenance. Figure 44 shows an example of the LW installations.

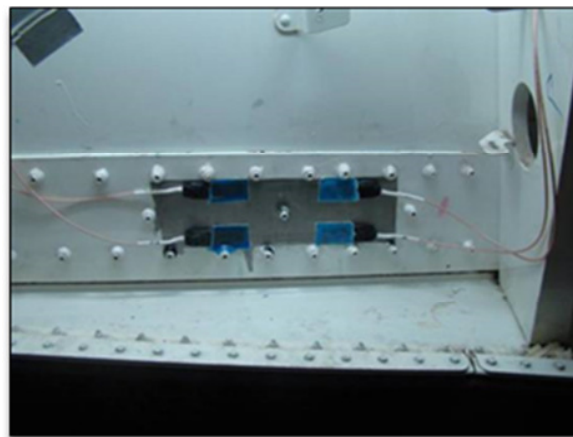


Figure 44 – LW Sensors Applied to the E-Jets Full-Scale Fatigue Test.

*Flight Tests with CVM Technology:* In order to verify if the CVM technology is capable of withstanding the real aircraft in-flight conditions, the next step after testing CVM in the FSFT, was to have CVM sensors and cables installed in an Embraer-190 flight test aircraft (Figs. 45 and 46) for periodic monitoring on ground.

The inspections were performed approximately every four months, using CVM ground equipment (the PM200 equipment from Structural Monitoring Systems Ltd). No cracks were detected (as expected); however, valuable information was gathered about sensors, cables and connectors.



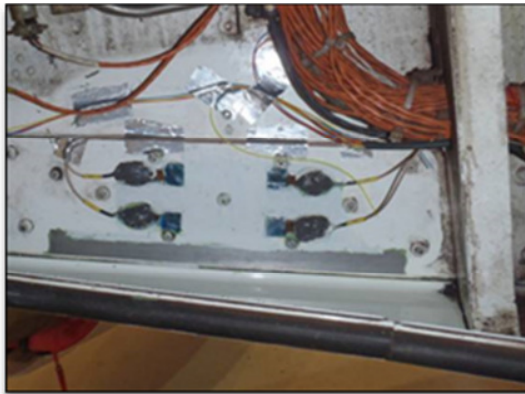
Figure 45 – Flight Test Aircraft Where CVM and LW Sensors Were Installed.



Figure 46 – Examples of CVM Sensors Installed in the Flight Test Aircraft.

*Flight Tests with Lamb Waves Technology:* Also for LW technology, the next phase after the FSFT was the field application in the flight tests. This phase is under development and it is aiming the evaluation of system and sensors in real operation, in order to demonstrate the ability of the Lamb Waves system to withstand the aircraft environmental and operational conditions. In addition, this phase intends to address the questions related to the sensors and cables durability.

Sensors were installed in the flight test aircraft Embraer-190 (Fig. 47). In this study, only the sensors and the cables are installed in the aircraft and the inspections/monitoring are performed periodically using ground support equipment.



(a)



(b)

Figure 47 – LW Sensors Applied to Flight Tests, Embraer-190 Aircraft. (a) Trailing Wing Box; (b) Passenger Door.

In another paper from R. Rulli, F. Dotta, C. G. Bueno and P. A. Silva (Ref. [24]), besides the SHM technologies above discussed, the authors report their experience with acoustic emission (AE) systems that have been tested by Embraer in test specimens and in the Full-Scale Fatigue Test of the E-Jets aircraft. These tests have the objective to provide enough information about Acoustic Emission technology regarding capabilities, installation, operation and maintenance of sensors and systems. Damages, including simulated and real, were satisfactorily detected by the AE systems in different test articles.

Figures 48 and 49 show some examples of application of AE in the FSFT, barrel test and coupon tests.

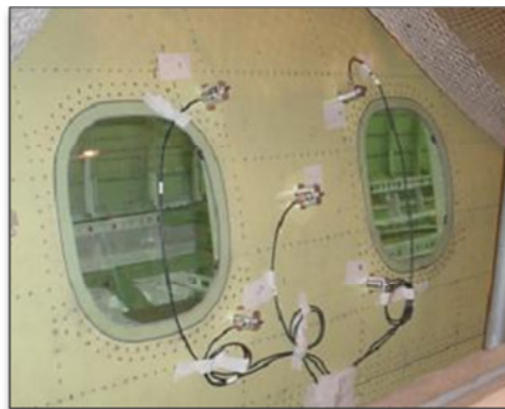


Figure 48 – Fuselage Panel in the E-Jets FSFT Monitored by Acoustic Emission.



(a)



(b)

Figure 49 – Examples of Acoustic Emission: (a) Barrel Test; (b) Coupon Test.

Finally, a paper written by L. G. dos Santos (Ref. [25]) presents a discussion about the challenges that an original equipment manufacturer (OEM) such as EMBRAER may face to introduce scheduled structural health monitoring (S-SHM) applications in the maintenance programs of its commercial aviation aircraft models. The following is a summary of L. G. dos Santos paper's discussion.

S-SHM solutions have the potential to contribute reduce aircraft operators direct maintenance costs and fleet downtime while keeping aircraft airworthiness at a minimum maintenance downtime and costs. As part of new approach in terms of scheduled maintenance practices, the replacement or complementation of traditional structural inspections tasks by new maintenance procedures taking credit of SHM technologies must be done in ways that meet the expectations and requirements of Regulatory Authorities, OEMs and airlines maintenance and engineering departments related to topics such as: safety, continued airworthiness, cost/benefits ratio, S-SHM systems' built-in redundancies and reliability to support higher fleet availability, as well as necessary mechanics qualification.

Besides the efforts for validation, verification, qualification and certification of such systems as able to deliver the expected effectiveness levels to verify structural integrity and withstanding the operational conditions to which it will be exposed, an OEM intended to offer their customers with the benefits of S-SHM solutions will be required initially to revise its policy and procedures handbooks (PPH) to adopt the new S-SHM Air Transport Association's Maintenance Steering Group 3 (MSG-3) Methodology guidelines.

This will alter in different ways the current Maintenance Review Board processes conducted by each OEM to develop and revise the minimum scheduled maintenance program for a given commercial aircraft type certificate. The contents of the Maintenance Review Board Reports (MRB) will need to be revised in order to clearly indicate the scope and frequencies of each approved S-SHM task, and how they will replace, complement

and/or be an alternative means of compliance of the more traditional maintenance tasks types such as general and detailed visual inspections (GVI and DET, respectively). Additionally, the Airplane Maintenance Manuals (AMM) will need to be revised to include specific S-SHM procedures on how to perform the intended inspection, how to proceed when degradation is detected in the monitored structures and how to repair such systems in case of failures.

## 8. REPAIRS

Regarding repairs, a paper from Pastoukhov, Baptista and co-workers (Ref. [25]), from University of São Paulo (USP), brings a proposal for the optimization of numerical analyses for maintenance of fuselage skins with typical rectangular repairs.

This approach, based on new crack growth simulations for worst case scenarios that could occur at the region of repair, uses respective kinetic equation and new geometric stress intensity factor functions, obtained in additional FEM analyses.

In particular, for standard rectangular repairs, the number of possible geometric configurations is very high considering length, width, skin and “doubler” thickness, reinforced panel dimensions, and frame and stringer cross sections.

This investigation deals mainly with defining a minimum sufficient number of intermediate crack length values for FEM analyses in each propagation scenario. A conservative but efficient definition of most relevant parameters for a new numerical analysis campaign is another important issue addressed in this work. The results obtained may be helpful for the improvement of the operational efficiency and safety of an aging fleet.

## 9. MISCELLANEOUS

**The LISA Project:** the LISA (Lightweight Integral Structures for Future Generation Aircrafts) Project is a cooperation work that is being carried out during the last years with Embraer and HZG. The main focus of this project is the investigation of FSW, laser modification and friction surfacing, with the purpose to improve the damage tolerance behavior of stiffened aluminium structures.

A work presented by Dr. N. Huber and co-workers, from HZG, (Ref. [27]) during the ICAF 2013 Conference, which demonstrates that the laser heating process is an interesting new approach for fatigue life enhancement or, more specific, for fatigue crack growth retardation, is part of the LISA project.

The LISA project is underway, and future works resulting from it are expected for the next years.



A Review of Aeronautical Fatigue  
Investigations in Brazil  
ICAF 2015 – Helsinki - Finland



## 10. REFERENCES

1. Rodengen, J. L., The History of Embraer, Write Stuff Inc., 2009.
2. Andrade, R. P. Aircraft Building: a Brazilian Heritage, 2008.
3. Argôlo, H. S. , Proença, S. P. B., *Generalized Finite Element Method and Splitting Method as a Framework for Multisite Damage*. The Third International Conference on Computational Modeling of Fracture and Failure of Materials and Structures, CFRAC2013, Prague, Czech Republic, 2013.
4. Carunchio, A. F. , Driemeier, L., Ramos Jr., R., Almeida, R. Z. H., Mendonça, W.R.P., *Numerical and Experimental Analysis of Riveted Joints for Aeronautical Applications*, 22<sup>nd</sup> International Congress of Mechanical Engineering, COBEM 2013 - Ribeirão Preto, Brazil, November 3-7, 2013.
5. Gamboni, O. C., Moreto, J. A., Bonazzi, L. H. C., Ruchert, C. O. F. T., Bose Filho, W. W., *Effect of Salt-water Fog on Fatigue Crack Nucleation of Al and Al-Li Alloys*, Materials Research. 2014; 17(1): 250-254.
6. Bonazzi, L. H. C., *Al-Li AA2050 Alloys Fatigue Behavior*, MsC Dissertation (in portuguese), 2014. University of São Paulo.
7. Pascoal, F. A. J., *Microstructural Analysis, Fracture Toughness and Fatigue Life in Alloys AA7050-T7451 and AA2050-T84*, MsC Dissertation (in portuguese), 2014. University of São Paulo.
8. Maciel, C. I. S., *Estudo Da Tenacidade E Fadiga Em Meio Assistido da Liga de Al-Li de Grau Aeronáutico AA 2050-T84*, MsC Dissertation (in portuguese), 2013. University of São Paulo.
9. Chemin, A., Spinelli D., Bose Filho, W. W., Ruchert, C. O. F. T., *Corrosion Fatigue Crack Growth Of 7475 T7351 Aluminium Alloy Under Flight Simulation Loading*, Procedia Engineering 101 ( 2015 ) 85-92.
10. Assunção, C. M., Chaves, C. E., *Experimental Determination of the Crack Tip Stress Intensity Factor in Integrally Stiffened Panels*, ICAF 2015, Helsinki, Finland, June 3-5, 2015.
11. Rodrigues, M. R. B., Fernandez, F. F., Miyazaki, M., *Fuselage Technology Demonstrator*, ASM - Aeromat Conference, Orlando – FL, USA, June 16-19, 2014.
12. Spangel, S., Miermeister, M., Gijbels, J., Fernandez, F. F., Nunes, D. F. S. , Miyazaki, M., *Manufacturing of an Advanced Wing Spar by FSW*, ASM - Aeromat Conference, Orlando – FL, USA, June 16-19, 2014.
13. Donadon, M. V., Arbelo, M. A., Contini, R., Gouvea, R., Arakaki, F. K., *An Experimental Study on the Durability of Stiffened Composite Panels with Skin/Stiffener Initial Flaws in the Post-Buckling Regime*, International

14. Endo, B. L. R. D., Donadon, M. V., Sales, R. C. M., Arakaki, F., *Characterization of Interlaminar Fracture Toughness with Thermo-Mechanical Effects of a Carbon Fiber-Epoxy Composite Material*, 2<sup>nd</sup> Brazilian Conference on Composite Materials – BCCM2, São José dos Campos – SP, September 14-18, 2014.
15. Sales, R. C. M., Gimenes, C. N., Guimarães, F., Marlet, J. M. F., Donadon, M.V., *Mixed Mode I+II Interlaminar Fracture Toughness of Reinforced Carbon Laminates Manufactured by VaRTM and HLUP: A Comparative Study*, 2<sup>nd</sup> Brazilian Conference on Composite Materials – BCCM2, São José dos Campos – SP, September 14-18, 2014.
16. Shiino, M. Y., Alderliesten, R. C., Donadon, M. V., Voorwald, H. J. C., Cioffi, M. O. H., *Applicability of Standard Delamination Tests (Double Cantilever Beam and End Notch Flexure) for 5HS Fabric-reinforced Composites in Weft-dominated Surface*, Journal of Composite Materials, September, 2014.
17. Donadon, M. V., Lauda, D. P., *A Damage Model for the Prediction of Static and Fatigue-Driven Delamination in Composite Laminates*, Journal of Composite Materials, Vol.1, pp. 01-13, 2014.
18. Ancelotti Jr., C., Noronha Melo, M. L. M., Gonçalves, V. O., Garcia, K., Pardini, L. C., *Experimental Methodology for Limit Strain Determination in a Carbon/epoxy Composite under Tensile Fatigue Loading*, Materials Science Forum, Vol. 805, pp. 311-318, 2015.
19. Souza, C. A. O., *Análise de Tensões e Vida em Fadiga de Juntas Coladas em Estruturas Aeronáuticas Metálicas*, PhD Thesis (in portuguese) University of Campinas (Unicamp), July, 2013.
20. Bürger, D., *Mixed-Mode Fatigue Disbond on Metallic Bonded Joints*, PhD Thesis, TU-Delft, March, 2014.
21. Bürger, D., Rans, C. D., Benedictus, R., *Characterization of Mixed-mode Fatigue Failure on Metallic Bonded Joints*. In ICAF 2013 Symposium - Proceedings of the 27th Symposium of the International Committee on Aeronautical Fatigue, pages 751-760, 2013.
22. Dotta, F., Ceresetti, L. B., *Evaluation of the Lamb Waves Approach to Detect Simulated Damage in an Orthogonal Plane of the Sensor Network Surface for Corrosion Detection Application*, Proc. of SPIE Vol. 8695 (2013) 86951L-1.
23. Rulli, R. P., Dotta, F., Silva, P.A., *Flight Tests Performed by EMBRAER with SHM Systems*, Key Engineering Materials, Vol. 558 (2013), pp. 305-313.
24. Rulli, R. P., Dotta, F., Bueno, C. G. G., Silva, P.A., *Damage Detection Systems for Commercial Aviation, on Smart Material Systems and Structures – Vol. 1 - Concepts and Applications*, to be Published.

25. Santos, L. G. dos, *Embraer Perspective on the Challenges for the Introduction of Scheduled SHM (S-SHM) applications into Commercial Aviation Maintenance Programs.*, Key Engineering Materials, Vol. 558 (2013), pp 323-330.
26. Pastoukhov, V., Baptista, C. A. R. P., Teixeira Jr., H. S., 3, Manzoli, P. R., *Optimization of Numerical Analyses for Maintenance of Fuselage Skins with Rectangular Repairs*, Advanced Materials Research Vols. 891-892 (2014) pp 615-620.
27. Schnubel, D., Horstmann, M., Huber, N., *Retardation of Fatigue Crack Growth in Aircraft Aluminium Structures via Heating Induced Residual Stresses – Experiments, Numerical Prediction and Design Optimisation*, In ICAF 2013 Symposium - Proceedings of the 27th Symposium of the International Committee on Aeronautical Fatigue, 2013.